Green Chemistry

CRITICAL REVIEW

View Article Online
View Journal | View Issue

Cite this: *Green Chem.*, 2019, **21**, 3744

Zeolite-supported metal catalysts for selective hydrodeoxygenation of biomass-derived platform molecules†

Wenhao Luo, *[a] Wenxiu Cao,[b] Pieter C. A. Bruijnincx,[c] Lu Lin,[a] Aiqin Wang *[a,d] and Tao Zhang*[a,d]

Increasing demand for renewable chemicals and fuels has stimulated the search for alternative feedstocks and is driving the ongoing transition to a more renewables-based society. Considerable academic efforts have been directed at the valorisation of biomass sources and derived intermediates, so called platform molecules, to produce value-added chemicals and fuels. In this contribution, opportunities are discussed for the application of zeolite-supported bifunctional catalysts in the conversion of biomass sources into chemicals and fuels *via* hydrodeoxygenation (HDO). Such metal/zeolite catalyst systems play a prominent role in many of these biomass HDO routes. Emphasis is put on the current progress in metal/zeolite-catalysed HDO of three selected, promising routes involving biomass-derived platform molecules and the model compounds that mimic more complex feeds. Four key concepts of metal/zeolite catalysts, such as combining metal and Brønsted acid sites, site-ratio balancing, proximity between metal and acid functions and shape selectivity are discussed in order to provide a comprehensive overview. In addition, two challenges related to the accessibility of the active sites and catalyst stability in the liquid phase, typically a hot, highly polar, and protic reaction medium, are discussed. Finally, the open challenges and perspectives regarding the development of metal/zeolite catalysts for biomass HDO reactions are examined.

Received 13th April 2019,
Accepted 3rd June 2019

DOI: 10.1039/c9gc01216h

rsc.li/greenchem

Introduction

The ever increasing energy and chemical demand, the accumulation of CO_2 in the atmosphere, price fluctuations and dwindling supplies of cheap and easily extracted petroleum, and the legislation and mandates that are the result of this, have all prompted the wide-ranging search for alternative feedstocks and technologies, a development that drives the essential transition to a more sustainable, renewables-based society.[1–5] Biomass is one promising renewable alternative that can serve as feedstock for the production of the fuels and chemicals that our society relies on. For energy supply in particular, the percentage of biomass used for renewable energy and carbon-based energy vector production is gradually growing in many countries at the expense of traditional fossil fuels. Similarly, exciting developments can be seen regarding biomass-to-chemicals, with routes and processes to both drop-in (*i.e.* molecularly identical) and new bio-based chemical building blocks being developed. Drop-in replacements hold the advantage of being compatible with current fossil fuel-based technology and value-chains, with the final products serving established markets. Nevertheless, for chemicals that are identical to the current petroleum-derived chemicals it is difficult to be economically competitive, given that there is little premium on green and that current petrochemical processing infrastructure has already been paid for. New bio-based oxygenated molecules may be difficult to be produced from petroleum feedstock and can hold unique properties, with applications in polymers, solvents, surfactants and pharmaceuticals. Nevertheless, the market for those new bio-based molecules has not yet been established and needs to be developed. Regardless if the targeted final product is new or existing, the most pursued strategy for biomass valorization to chemicals is, analogously to the current petrochemical industry, to first upstream fractionate and/or deconstruct the complex, polymeric biomass matrix to give so-called platform molecules, *i.e.*

[a]*CAS Key Laboratory of Science and Technology on Applied Catalysis, Dalian Institute of Chemical Physics, Chinese Academy of Sciences, 457 Zhongshan Road, Dalian,116023, China. E-mail: w.luo@dicp.ac.cn, aqwang@dicp.ac.cn, taozhang@dicp.ac.cn*
[b]*College of Chemistry and Chemical Engineering, Jishou University, Jishou, Hunan 416000, China*
[c]*Organic Chemistry and Catalysis, Debye Institute for Nanomaterials Science, Utrecht University, Universiteitsweg 99, 3584 CG Utrecht, The Netherlands*
[d]*State Key Laboratory of Catalysis, Dalian Institute of Chemical Physics, Chinese Academy of Sciences, Dalian 116023, China*

† Dedicated to Dalian Institute of Chemical Physics, CAS, on the occasion of its 70th anniversary.

molecularly well-defined and versatile chemical building blocks, from which chemical complexity can be built up downstream to yield a plethora of platform molecule-derived value-added products. Indeed, while many different biomass resources, fractionation methods and catalytic conversion routes are explored for the production of tailor-made chemicals and fuel components,[6] many of these feature the same, small group of valuable chemical intermediates with the potential to play a pivotal role as primary biorefinery building blocks.[7,8] The basic chemical building blocks that currently serve as platform molecules, in fossil fuel-based refineries, are normally apolar, non-functionalized and low reactivity hydrocarbon compounds, and upgrading these requires the activation of the C–C and C–H bonds of these intermediates to build up the complexity of the carbon skeleton and to introduce the heteroatoms and functional groups, *e.g.* by oxygenation, required for value-added chemicals and fuels production. Many of the catalytic reactions involved in these processes make use of zeolites; these solid acid catalysts are the workhorses of the petrochemical industry and oil refining, being used in large volumes also in processes such as hydrocracking and fluid catalytic cracking.[9–11] On the contrary, biomass-derived platform molecules are usually polar, highly reactive and extensively functionalized oxygenates, and partial deoxygenation by activation and cleavage of C–O and C=O bonds is typically involved in further upgrading. Such deoxygenation reactions then involve a combination of hydrolysis, dehydration and reduction steps in the conversion sequence, reactions which if the intermediates involved are fairly stable, can be performed separately (*i.e.* in different reactors) by multiple catalyst systems or in one-pot; if the intermediates are rather unstable or thermodynamically unfavorable, however, as is often the case for the conversion of biomass-derived oxygenates in biorefinery processes, such consecutive conversions are preferably closely coupled, *e.g.* by using catalysts that combine different functionalities in one and the same material. For reactions requiring acidity and hydrogenation activity, zeolites, by virtue of their high surface area, porosity, chemical and hydrothermal stability, and Brønsted acidity, are particularly useful for constructing such bifunctional materials *e.g.* by inclusion of redox-active metal sites. To tailor the product distribution, efficient coupling of the different reactions involved is then required, which can be realized *via* optimization of the site-ratio of the different catalytic functions. If the Brønsted acid and hydrogenation functions are then put in close proximity, synergistic effects can be expected. Indeed, the 'closer-the-better' in terms of positioning the acid and metal sites is often advocated as being advantageous for the activity and selectivity of bifunctional catalysts,[12–15] although the opposite has unexpectedly been demonstrated for the industrially highly important hydrocracking reaction.[10] Building on the precedent of commercial application in oil refining, bifunctional zeolite-supported metal catalysts are now also being quite extensively studied for the valorization of renewable feedstocks such as biomass and its platform molecules.[16–18]

In this review, we highlight the recent developments and current state of the art of the application of metal/zeolite catalysts for the conversion of biomass into chemicals and fuels. We first present the catalyst design principles that have been employed for biomass conversion, and focus on the hydrodeoxygenation (HDO) of selected platform molecules central to biomass downstream processing and model compounds mimicking some more complex feeds that are upgraded downstream by HDO, and thus cover the examples of HDO of levulinic acid, phenolics and triglycerides and fatty acids. The emphasis of the review is on four prominent concepts and two new challenges (Fig. 1). Concepts key to metal/zeolite catalysis, referring to combination of metal and Brønsted acidity, site-ratio balancing, intimacy/proximity between metal and acid functions and shape selectivity, are introduced and high-

Wenhao Luo

Wenhao Luo, born in 1984 in Jilin, China, obtained his PhD (2014) under the supervision of Prof. Bert Weckhuysen and Prof. Pieter Bruijnincx from Utrecht University in 2014 on the rational design and exploitation of bifunctional catalysts for hydrodeoxygenation of bio-derived platform molecules. Afterwards, he worked as a post-doctoral fellow in the group of Prof. Johannes Lercher at Technical University of Munich. In 2016, he joined Prof. Tao Zhang's group as an associate professor, and his research interest focuses on rational design of bifunctional catalysts, for catalytic biomass valorization and C1 chemistry.

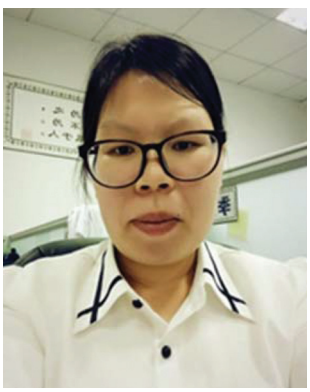

Wenxiu Cao

Wenxiu Cao received her PhD (2012) under the supervision of Prof. Yingwei Li from South China University of Technology, Guangzhou, China. After receiving her degree, she joined Shaanxi University of Technology as a lecture in 2012. In 2015, she worked as a post-doctoral fellow for two years in Prof. Tao Zhang's group in Dalian Institute of Chemical Physics (DICP). In 2017, she returned to Shaanxi University of Technology. In 2018, she moved to Jishou University to work as a lecturer. Her research interest focuses on the stability and application of bifunctional catalysts in biomass transformations.

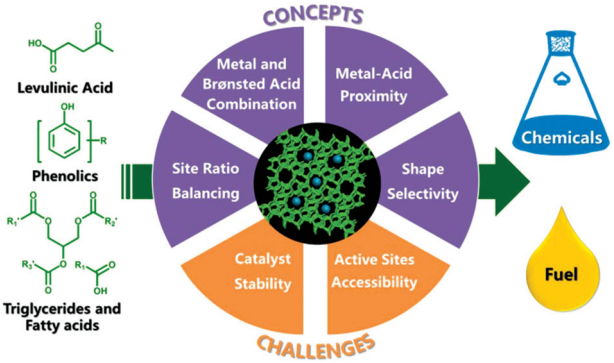

Fig. 1 Concepts and challenges of zeolite-supported metal catalysts for hydrodeoxygenation of biomass-derived platform molecules.

lighted with specific examples. Challenges relating to the accessibility of the active site and catalyst stability in the highly polar, and often protic liquid phase are demonstrated in detail. Finally, the recent advances in zeolite-supported bifunctional catalysis for the HDO of the selected biomass-derived platform and model compounds will be highlighted, reflecting on the existing gaps and perspectives with respect to catalyst development.

Design principles of metal/zeolite catalysts

HDO of biomass-derived platform molecules into chemicals and fuels often requires a cascade of reactions, including hydrolysis, dehydration and hydrogenation steps and as result a catalyst that offers activity in these different reactions. Therefore, rational combination of metal and acid sites is pivotal in catalyst design. Zeolites have become the most prominent acid catalysts and been widely applied in HDO reactions. Various techniques are employed for the introduction of different metals into zeolites in biomass conversion (Table 1). Only metal clusters and nanoparticles will be discussed here, which thus excludes the single-atom/zeolite system and metals substituting lattice atoms in the zeolite framework. Different preparation methods for metal/zeolite catalysts used in HDO reactions of biomass platform molecules are listed in Table 1.

Dry or wet-impregnation with a metal precursor is most widely used for the preparation of metal/zeolite catalysts. Specifically, this impregnation technique normally consists of mixing a zeolite support with the required amount of metal precursor solution. The volume amount of the solution is equal to the total pore volume of the support in dry impregnation or larger than that of the support in wet impregnation. Solutions of various metal precursors, such as nitrate, chloride or carboxylate salts, are usually employed, to fill the pores and obtain a homogeneous metal distribution. Nevertheless, the diffusion of the impregnation solution into small micropores is difficult, especially when residual gas is present in the micropores and when the support is poorly wetted by the solution. In addition, impregnated precursors are only weakly anchored onto the zeolite surface and thus redistribute and agglomerate during the subsequent typical calcination and reduction treatments. Therefore, this preparation method is usually not best suited for achieving high metal loadings and uniform metal dispersions, and the metal frequently disperses in a nonuniform style, producing large particles on the external surface of the zeolite.

Alternatively, ion exchange is a technique often used to load metals into the micropores of zeolites. This synthesis technique normally consists of cation exchange in dilute aqueous solutions containing the metal cations, filtration and washing off, calcination and reduction steps. During the ion exchange process, the pH value should be carefully adjusted to avoid precipitation of the metal cations. The exchange processes are usually conducted by one exchange step at room

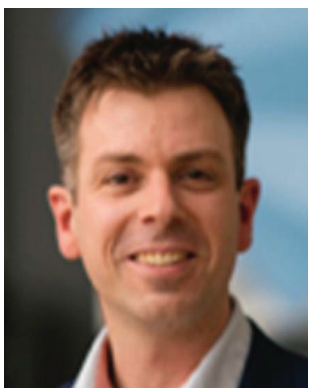

Pieter C. A. Bruijnincx

Pieter Bruijnincx obtained his PhD degree from Utrecht University (2007, highest honors). After a postdoctoral stay at Warwick University, he returned to Utrecht in 2009 as assistant professor to work on catalytic biomass conversion. He currently is full professor of Sustainable Chemistry and Catalysis. His main research interests lie in the development of new heterogeneous and homogeneous catalysts and novel conversion routes for sustainable production of chemical building blocks from biomass, CO_2 or waste streams as well as the development of new concepts in molecular catalysis.

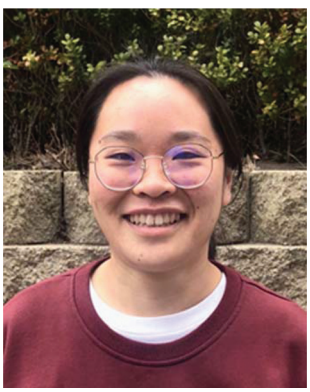

Lu Lin

Lu Lin obtained her PhD (2017) under the supervision of Prof. Xiongfu Zhang from Dalian university of Technology, China on the development of MOF-coated core–shell catalysts. In 2018, she joined Dalian Institute of Chemical Physics (DICP), to work as a postdoctoral fellow in Prof. Tao Zhang's group. Her research interest focuses on the design and application of MOF-based bifunctional catalysts in biomass transformations and C1 chemistry

Table 1 Preparation methods of metal/zeolite catalysts for HDO reactions of bio-derived platform molecules

Preparation methods	Process steps	Advantages	Limitations
Impregnation (dry and wet)	Impregnation-drying-calcination-reduction	Generally and easily applicable, access to high metal loadings.	Weak metal-support interaction; metal migration out of pores, resulting in formation of large particles at external surface of zeolite upon heat treatment; sintering in liquid phase
Ion exchange	(Multi-step) exchange-filtration-drying-calcination-reduction	Highly dispersed and homogeneous distribution, strong metal-support interaction	Metal should be available in cation form; cation needs to be stable at a pH value where zeolite is also stable; complex cations should be smaller than zeolite pore size; not applicable with neutral framework materials such as aluminophosphates and silicalite; dilute solution is preferred and metal loading cannot surpass exchange capacity
Combination of wet impregnation and ion exchange	Impregnation/exchange-drying- (calcination) reduction	Highly dispersed and homogeneous distribution, strong metal-support interaction	Some metal particles form at external surface of zeolite upon heat treatment
Melt infiltration	Melt impregnation-calcination-reduction	No solvent required, high dispersions can be achieved	The metal precursor should be completely molten at appropriate temperature; weak metal-support interaction; some large particles may form and agglomerate on the external surface of the zeolite upon heat treatments
Deposition-precipitation (DP)	Precipitation-filtration-drying-calcination-reduction	Uniform distribution of metal nanoparticles, and effective for low metal loadings and high Si/Al ratio zeolites	Metal nanoparticles mainly form and locate at external surface of zeolites
Atomic layer deposition (ALD)	Outgassing-vapor pulsing-deposition-purge	Excellent uniformity, precise thickness control at the Ångstrom or monolayer level with high reproducibility.	The metal precursor should be vaporizable and molecular dimensions cannot surpass a critical size to penetrate and diffuse into the pore structure
In situ encapsulation/ confinement synthesis	Metal precursor addition during synthesis of zeolite-crystallization-calcination-reduction	Included metal clusters/particles are resistant to sintering, show high thermal stability.	Low aluminum content zeolites required due to crystallization requirements

temperature, while higher levels of exchange require multiple exchange steps in fresh solutions, and the use of higher temperatures can favour the kinetics of the exchange. While this technique is good for obtaining highly dispersed small metal clusters into the pores of zeolites, it can not be successfully applied in the following situations, (1) when the metal is in anionic form, or metal cations are only stable under conditions where zeolites are unstable, for example, very low pH value; (2) when the zeolite/zeotype framework is neutral (aluminophosphates) or aluminium-free (silicalite); (3) when the

Aiqin Wang

Aiqin Wang, received her PhD degree of physical chemistry from Dalian Institute of Chemical Physics (DICP) in 2001. She joined Prof. Tao Zhang's group where she was promoted to a full professor in 2009. She became a joint professor of State Key Laboratory of Catalysis in 2013 and chair professor in 2017. Her research interests include catalytic conversion of biomass, subnano- and single-atom catalysts, and green synthesis of value-added chemicals. She has co-authored over 270 peer-reviewed publications, and serves as an editorial board member of Chinese Journal of Catalysis and an Advisory Board member for Sustainable Energy and Fuels.

Tao Zhang

Tao Zhang, currently the vice president of the Chinese academy of sciences, received his PhD in physical chemistry from Dalian Institute of Chemical Physics (DICP) in 1989. He was promoted to full professor of DICP (1995), the director of DICP (2007–2017), and Academician of the Chinese Academy of Sciences (2013). He received several research awards, including the Science and Technology Progress Award of HLHL Foundation (2016), Distinguished Award of Chinese Academy of Sciences (2010), Zhou Guang Zhao Foundation Award for Applied Science (2009), Excellent Young Scientist Award of Chinese Catalysis Society (2008), and National Award of Technology Invention (2008, 2006, 2005).

target metal loading is above the upper limit of exchange capacity, which depends on the amount of framework aluminium and finally, (4) when the metal complex cations are bigger than the pore system.

A combination of wet impregnation and ion exchange (modified wet impregnation) method has recently been applied for the synthesis of platinum-group metal/zeolite catalysts.[13] This method typically employs $Pt(NH_3)_4^{2+}$, $Ru(NH_3)_6^{3+}$, $Pd(NH_3)_4^{2+}$ cations for impregnation/exchange with the proton or ammonium form of zeolites, after which the slurry of the zeolite and the metal cation-containing solution is dried directly at elevated temperature without filtration, followed by calcination and reduction to finally generate the supported metal particles. Highly dispersed metal clusters can thus be obtained, located even partly in the micropores, *via* this simple combination of techniques, but when the targeted metal loading is beyond the exchange capacity, this technique has the same limitations as the wet impregnation methods.

Metal infiltration is another versatile technique for the preparation of transition metal loaded zeolite catalysts.[19] Generally, hydrated transition metal nitrates with low melting points are used in such melt infiltration approaches. The molten metal salts infiltrate and enter into the zeolite pores as a result of capillary forces. Importantly, the melt temperature needs to be finely adjusted to prevent decomposition of the metal precursor during the whole process. High dispersion of the metal can be achieved owing to the avoidance of adding a large amount of solvent molecules, such as water, which may competitively adsorb on the surface of the zeolite support.

Deposition-precipitation (DP) has also been employed for metal/zeolite synthesis, in particular when higher loadings are targeted.[20,21] Typically, this method entails the precipitation of a metal onto zeolite support by basification of a metal salt solution containing zeolite in suspension through decomposition of urea. After a chosen DP time (typically 1–4 h), the suspension is cooled, filtered and washed multiple times, followed by drying, calcination and reduction steps. Generally, high metal loadings and metal dispersions can be achieved *via* DP, with the metal nanoparticles being mainly located on the external surface of the zeolite.

Atomic layer deposition (ALD) has also been employed for the metal/zeolite synthesis.[22,23] Typically, the vaporized metal precursor is introduced to a fully outgassed zeolite in the reaction chamber by pulsing with an inert carrier gas, allowed to deposit for a few seconds, after which the system is purged to remove the residue precursor after deposition. The metal loading can be varied by changing the ALD cycle numbers. Precise control of metal layer at the Ångstrom or monolayer level could be exerted, with the metal being on the external surface with high reproducibility, however, the metal precursors should be easily vaporized and their molecular size should be small enough for penetrating and diffusing facilely into the porous structure of zeolite.

In situ encapsulation/confinement synthesis technologies have also been reported for the preparation of metal/zeolite catalysts recently.[24–27] Typically, a metal precursor is introduced during zeolite synthesis or structure transformation, followed by crystallization, calcination and reduction. Well-dispersed and ultra small metal clusters can be encapsulated into zeolites *via* this method; however, the zeolites prepared *via* this technique often contain a low amount of aluminium, as larger aluminium contents are unfavorable for the crystallization/structure transformation process.

All the above mentioned preparation techniques have been employed for the synthesis of metal/zeolite bifunctional catalysts, and are being more and more frequently applied in biomass conversion. However, the location of metal species cannot always be controlled, and metal nanoparticles (NPs) will usually be formed upon post-treatment. Moreover, upon application in the liquid phase reaction or as a result of harsh thermal treatments, metal species on the external surface can aggregate to form large NPs (>5 nm), resulting in a decrease in catalytic activity. In addition, the rational design of ideal metal/zeolite bifunctional catalysts with an optimal balance and ratio of distinct sites still requires further exploration for the various HDO reactions. Especially, to develop the ability to achieve the right proximity and as a result synergy between the metal and the acid sites confined inside the zeolite micropores would have much potential in catalyst design and can improve the efficiency of upgrading through HDO. Indeed, efficient coupling of the involved tandem reactions can allow one to tune product distribution and improve the selectivity towards desired products. In addition to improved activity and selectivity, other synergy effects can be expected, *e.g.* with regards to catalyst stability, since an increase in interaction between metal and acid inside micropores of zeolite can limit or eliminate metal migration, sintering and leaching during heat treatment or liquid phase reactions.

Concept 1: combining metal and Brønsted acid functions

Deoxygenation is often essential in the upgrading of biomass-derived oxygenates to biofuels and chemicals. For example, bio-oils produced *via* catalytic pyrolysis of lignocellulosic biomass, having undesirable physicochemical properties and being chemically unstable, requires further catalytic upgrading to be used as fuels as such or to be blended into today's petroleum-based infrastructure. Interest in this subject of catalytic upgrading by deoxygenation has been growing rapidly in recent years. Most of the catalytic deoxygenation reactions have been performed with heterogeneous catalysts and under conventional hydrotreating conditions. The performance of various metal/zeolite catalysts for HDO of biomass-derived platform molecules (levulinic acid, phenolics and triglycerides and fatty acids) is summarized, and details are given in Tables 2–4.

Bifunctional catalysis with sugar-derived levulinic acid

Levulinic acid (LA), known as 4-oxopentanoic acid or 4-ketopentanoic acid, is one of the most explored and promising bio-

Table 2 HDO platform of LA with metal/zeolite catalysts

Catalyst (Si/Al)	Solvent	Feed	T (K)	P (bar)	WHSV (h^{-1})	Time (h)	Major product (yield%)	Ref.
1 wt% Ru/H-ZSM-5 (11.5)	Dioxane	10 wt% LA	473	40	—	10	GVL: (31.3); PA + PE: (57.4)	13
1 wt% Ru/H-ZSM-5 (140)	Dioxane	10 wt% LA	473	40	—	10	GVL: (58.2); PA + PE: (1)	13
1 wt% Ru/H-ZSM-5 (11.5)	Dioxane	10 wt% LA	473	40	—	10	PA + PE (91.3); GVL (7.7)	13
30 wt% Ni/H-ZSM-5 (40)	No solvent	Neat LA	523	1	1.1	—	GVL (92.2)	40
5 wt% Ru/H-ZSM-5C (25)	Water	15 wt% LA	343	30	—	6	GVL (92.8)	45
5 wt% Ru/H-ZSM-5S (25)	Water	15 wt% LA	343	30	—	6	GVL (92)	45
5 wt% Ru/H-ZSM-5 M (25)	Water	15 wt% LA	343	30	—	6	GVL (95)	45
0.7 wt% Pt/H-ZSM-5/SiO_2	No solvent	Neat GVL	523	10	2	—	PA (> 80)	32
5% Pd/H-Y (2.6)[a]	Octane	38.4% GVL	533	80	—	30	Pentyl valerate (60.6); pentane (22.9)	47
5 wt% Pt/H-ZSM-5 (11)	No solvent	Neat LA	473	8	—	1	PA (78); GVL (15)	50
5 wt% Ir/H-ZSM-5 (11)	No solvent	Neat LA	473	8	—	1	PA (29); GVL (48)	50
5 wt% Pd/H-ZSM-5 (11)	No solvent	Neat LA	473	8	—	1	PA (5); GVL (47)	50
5 wt% Rh/H-ZSM-5 (11)	No solvent	Neat LA	473	8	—	1	PA (17); GVL (60)	50
5 wt% Ru/H-ZSM-5 (11)	No solvent	Neat LA	473	8	—	1	PA (30); GVL (59)	50
5 wt% Pd/H-ZSM-5 (15)	No solvent	Neat LA	473	8	—	1	PA (27); GVL (51)	50
5 wt% Pt/H-ZSM-5 (11)	Toluene	28 wt% LA	473	8	—	6	PA (83)	50
5 wt% Pt/H-ZSM-5 (11)	Mesitylene	28 wt% LA	473	8	—	6	PA (81)	50
5 wt% Pt/H-ZSM-5 (11)	Dioxane	28 wt% LA	473	8	—	6	PA (19); GVL (40)	50
5 wt% Pt/H-ZSM-5 (11)	Water	28 wt% LA	473	8	—	6	PA (73)	50
5 wt% Pt/H-ZSM-5 (11)	No solvent	LA	473	8	—	6	PA (99)	50
5 wt% Pt/H-ZSM-5 (11)	Ethanol	19 wt% LA	473	8	—	24	PE (75)	50
5 wt% Pt/H-ZSM-5 (11)	Methanol	28 wt% LA	473	8	—	3	PE (87)	50
0.15 wt% Pt/H-ZSM-5 (50)	Water	2% LA	473	10	—	3	PA (91.4); GVL (4.4)	23
0.46 wt% Pt/H-ZSM-5 (50)	Water	2% LA	473	10	—	3	PA (7.9); GVL (51.8)	23
10 wt% Co@H-ZSM-5 (38)	Ethanol	17% LA	513	30	—	3	PA + PE (>90)	51
10 wt% Ni/H-ZSM-5 (38)	Ethanol	16.7 wt% LA	513	30	—	3	PA + PE (90%)	52
10 wt% Ni/$K_{0.5}$/H-ZSM-5 (38)	Ethanol	16.7 wt% LA	513	30	—	3	PA + PE (>90%)	52
3.9 wt% Pt-0.13 wt% Mo/H-β	Water	3.7 wt% LA	403	50	—	12	MTHF (86%)	53

[a] The loading is not clear in wt% or mol%.

based short chain platform chemicals.[7,8] LA can be produced easily and economically from the C_6 sugar fraction of various lignocellulosic biomass feedstocks through a simple and high yielding acid hydrolysis process.[28–30] A whole slate of valuable chemicals, such as γ-valerolactone (GVL), 1.4-pentanediol (PD), 2-methyltetrahydrofuran (MTHF), pentenoic acid (PEA), pentanoic acid (PA) and its esters (PE) can be subsequently converted by sequential LA HDO steps, as depicted in Scheme 1. GVL has attracted most attention owing to its excellent properties as solvent and it being a building block for high-value chemicals and fuels.[31] Valeric acid ester biofuels, derived from PA/PE, have also received increasing attention owing to outstanding fuel properties, as evidenced by a successful road trial of 250 000 km.[32]

The LA-to-GVL step is readily catalyzed with various metal catalysts, including both noble (Ir, Rh, Pd, Ru, Pt, Re, Au) and non-noble metals (Ni, Co, Cu), at moderate reaction temperatures ranging from 298 to 523 K with hydrogen pressures of 1 to 150 bar.[33–41] LA can be transformed to GVL either *via* a first hydrogenation step to 4-hydroxypentanoic acid followed by dehydration or *via* dehydration to angelicalactone and subsequent hydrogenation (Scheme 1). For LA-to-GVL reactions run at elevated temperature range (>353 K), metal sites have shown a dominant impact on the rate of GVL formation, owing to the acid-catalyzed dehydration step aided by the relative high temperature. While at low temperature range (<353 K), the acid-catalyzed dehydration step appears to be the rate-determining step and dominate the rate of GVL formation.[42]

The presence of metal and Brønsted acid sites together can efficiently couple the hydrogenation and dehydration reaction cascade, leading to an increase in the reaction rate of HDO of LA. Such an increase in GVL production was for example demonstrated by combination of the ion exchange resin Amberlyst A70 with Ru/C.[43] Combining Brønsted acid sites and a hydrogenation metal in a bifunctional catalyst may be more desirable, however, than a physical mixture of two.[44] Zeolites are particularly suitable and used as support for the bifunctional catalysts, since they have already shown great potential in many Brønsted acid-catalyzed reactions. Indeed, various types of zeolites supported (H-ZSM-5, H-β and H-Y) metal catalysts have been applied and showed a superior high activity than the only metal catalysts, for dehydration steps of LA HDO.[45,46] For example, Ru/ZSM-5 (Si/Al = 25) catalysts showed higher LA conversion (>97%) and GVL yield (>91%) than Ru/TiO_2, Ru/Al_2O_3, Ru/SiO_2 (GVL yield <81%) for the HDO of LA at 343 K and 30 bar H_2 after 6 h reaction in aqueous solution.[45] Different preparation methods were compared for the Ru/ZSM-5 catalyst. Wet impregnation proved advantageous for the preparation of Ru/ZSM-5, when compared to a supercritical CO_2-assisted deposition method.

Also, using the same wet impregnation method, a commercial ZSM-5 supported Ru catalyst showed better stability in the liquid phase conversion of LA to GVL than a mesoporous

Table 3 HDO of phenolics over metal/zeolite catalysts

Catalyst (Si/Al)	Solvent	Feed	*T* (K)	*P* (bar)	WHSV (h^{-1})	Time (h)	Major product (yield %)	Ref.
1 wt% Pt/H-Y (6)	Water	90 wt% phenol	523	40	20	—	Cyclohexane (94); bicyclics (4)	67
1 wt% Pt/H-β	Water	90 wt% phenol	523	40	20	—	Cyclohexane (95); bicyclics (4)	67
1 wt% Pt/H-ZSM-5	Water	90 wt% phenol	523	40	20	—	Cyclohexane (87); bicyclics (1)	67
0.1 wt% Pd/H-β (75)	Water	6.6 wt% 4-*n*-propylphenol	523	50	—	2	Bicycloalkanes (77)	72
0.8 wt% Pd/20 wt% H-Y (2.8)–Al_2O_3	Octane	1 wt% phenol	523	15	0.5	—	Cyclohexane + cyclohexene (60)	68
9.3 wt% Ni/19.3 wt% Al_2O_3–ZSM-5 (90)	Water	5.9 wt% phenol	493	50	—	1.7	Cyclohexane (~18)	69
10 wt% Ni/H-ZSM5 (38)	Water	4.8 wt% phenol	513	40	—	3	Benzene (60); cyclohexane (23)	71
1 wt% Ru/H-ZSM-5 (25)	Water	2 wt% phenol	423	50	—	2	Cyclohexane (96)	63
1 wt% Ru/H-ZSM-5 (38)	Water	2 wt% phenol	423	50	—	2	Cyclohexane (87); cyclohexanol (10)	63
1 wt% Ru/H-ZSM-5 (50)	Water	2 wt% phenol	423	50	—	2	Cyclohexane (14); cyclohexanol (83)	63
1 wt% Ru/H-ZSM-5 (360)	Water	2 wt% phenol	423	50	—	2	Cyclohexanol (97)	63
1 wt% Pd/H-ZSM-5 (38)	Water	2 wt% phenol	423	50	—	2	Cyclohexane (73); cyclohexanol (24)	63
1 wt% Pt/H-ZSM-5 (38)	Water	2 wt% phenol	423	50	—	2	Cyclohexane (69); cyclohexanol (28)	63
1 wt% Ru/H-ZSM-5 (25)	Water	2 wt% anisole	423	50	—	2	Cyclohexane (93)	63
1 wt% Ru/H-ZSM-5 (25)	Water	2 wt% catechol	423	50	—	2	Cyclohexane (96)	63
1 wt% Ru/H-ZSM-5 (25)	Water	2.4 wt% guaiacol	423	50	—	2	Cyclohexane(94)	63
10 wt% Ni-10 wt% Co/H-ZSM-5 (17)	Water	4.8 wt% phenol	523	50	—	2	Cyclohexane (91); bezene(8)	64
21 wt% Ni/H-ZSM-5 (17)	Water	4.8 wt% phenol	523	50	—	2	Cyclohexane (85); benzene(8)	64
21 wt% Ni-21 wt% Cu/H-ZSM-5 (17)	Water	4.8 wt% phenol	523	50	—	2	Cyclohexane (63); cyclohexene (7)	64
17 wt% Ni-2 wt% Cu/H-ZSM-5 (17)	Water	4.8 wt% phenol	523	50	—	2	Cyclohexane (37); cyclohexene (4)	64
1 wt% Pt/H-ZSM-5 (45)	Water	2.4 wt% guaiacol	453	50	—	5	Cyclohexane (93)	73
1 wt% Pt/H-ZSM-5 (120)	Water	2.4 wt% guaiacol	453	50	—	5	Cyclohexane (53); methoxycyclehexanol (35)	73
0.5% Ru/H-β (13.5)	Water	5.9 wt% guaiacol	413	40	—	8	Cyclohexane (97)	62
0.5% Ru/H-β(13.5)	Water	7.6 wt% eugenol	413	40	—	8	Propylcyclohexane (95)	62
0.5 wt% Pt/H-Y (2.6)	Decane	7.5 wt% guaiacol	423	40	—	2	Cyclohexane (46)	74
0.5 wt% Pt/H-Y (2.6)	Decane	7.5 wt% anisole	423	40	—	2	Cyclohexane (86)	74
0.5 wt% Pt/H-Y (2.6)	Decane	7.5 wt% phenol	423	40	—	2	Cyclohexane (69)	74
0.5 wt% Pt/H-Y (2.6)	Decane	7.5 wt% veratrole	423	40	—	2	Cyclohexane (13); 2-methoxyphenol (32)	74
0.5 wt% Pt/meso-β (12.5)	Decane	7.5 wt% guaiacol	523	40	—	2	Cyclohexane (45); methylcyclopentane (15)	75
0.5 wt% Pt/meso-ZSM-5 (15)	*n*-Tridecane	3 wt% guaiacol	473	40	1–6	—	Hydrocarbon (50–98)	76
0.5 wt% Pt/meso-ZSM-5 (15)	*n*-Tridecane	3 wt% cresol	473	40	1–6	—	Hydrocarbon (>95)	76
0.5 wt% Pt/H-β (12.5)	Decane	7.5 wt% guaiacol	523	40	—	2	Cyclohexane (26), methylcyclopentane (13)	75
2.5 wt% Ru-2.5 wt% Cu/HY (2.6)	Water	3.3 wt% guaiacol	523	40	—	2	Cyclohexane (45); bicyclics (10)	77
2 wt% Pt/H-ZSM-5 (45)	Octane	12 wt% 4-propylphenol	383	1	—	10	Propylcyclohexane (99)	78
2 wt% Pt/H-ZSM-5 (45)	Octane	14.2 wt% methoxy-4-propylphenol	383	1	—	24	Propylcyclohexane (99)	78
2 wt% Pt/H-ZSM-5 (45)	Octane	12 wt% 2,4,6-trimethylphenol	383	1	—	24	Trimethylcyclohexane (91)	78
2 wt% Pt/H-ZSM-5 (45)	Octane	14 wt% 2-*tert*-butyl-6-methylphenol	383	1	—	24	*Tert*butylmethylcyclohexane (95)	78
2 wt% Pt/H-ZSM-5 (45)	Octane	18 wt% 2,6-di-*tert*-butyl-4-methylphenol	383	1	—	24	*Tert*butylmethylcyclohexane (45)	78
2 wt% Pt/H-ZSM-5 (45)	Octane	13 wt% methyl 4-hydroxybenzoate	383	1	—	24	Cyclohexanecarboxylate (67)	78
20 wt% Ni/H-ZSM-5 (45)	Water	Alkyl-, ketone-, hydroxyl-substituted phenols and guaiacols, alkyl-substituted syringol, (10 mmol) in 80 mL water	523	50	—	2	Cycloalkane (73–92); aromatic hydrocarbon (5–12)	79
1 wt% Ru/H-ZSM-5 (25)	Water	Phenolic dimers: 4-O-5, α-O-5, 5–5′, β-5, (2.0 mmol) in 10 mL water	473/493	50	—	4	Cycloalkane (>84)	63
0.5 wt% Ru/H-β (13.5)	Water	Phenolic dimers: 4-O-5, α-O-4, β-O-4, 5–5′ (2 mmol) in 4 mL water	413	40	—	3/8	Cycloalkane (93, 94, 65, 95)	62
20 wt% Ni/H-ZSM-5 (45)	Water	Phenolic dimers: β-O-4, (10 mmol) in 80 mL water	523	50	—	2	Cycloalkane (63); aromatic hydrocarbon (37)	79

Table 3 *(Contd.)*

Catalyst (Si/Al)	Solvent	Feed	*T* (K)	*P* (bar)	WHSV (h^{-1})	Time (h)	Major product (yield %)	Ref.
20 wt% Ni/H-ZSM-5 (45)	Water	Phenolic dimers: α-O-4, (10 mmol) in 80 mL water	523	50	—	2	Cycloalkane (82); aromatic hydrocarbon (18)	79
20 wt% Ni/H-ZSM-5 (45)	Water	Phenolic dimers: 4-O-5, (10 mmol) in 80 mL water	523	50	—	2	Cycloalkane (95); aromatic hydrocarbon (5)	79
20 wt% Ni/H-ZSM-5 (45)	Water	Phenolic dimers: 5–5′, (10 mmol) in 80 mL water	523	50	—	2	Cycloalkane (97); aromatic hydrocarbon (3)	79
20 wt% Ni/H-ZSM-5 (45)	Water	Phenolic dimers: β-1, (10 mmol) in 80 mL water	523	50	—	2	Cycloalkane (66); aromatic hydrocarbon (34)	79
20 wt% Ni/H-ZSM-5 (45)	Water	Phenolic dimers: β–β, (10 mmol) in 80 mL water	523	50	—	2	Cycloalkane (60); aromatic hydrocarbon (40)	79
20 wt% Ni/H-ZSM-5 (45)	Water	Phenolic dimers: β-5, (10 mmol) in 80 mL water	523	50	—	2	Cycloalkane (53); isomerized hydrocarbon (37)	79
2.5 wt% Ru-2.5 wt% Cu/H-Y (2.6)	Water	3.3 wt% diphenyl ether(4-O-5)	523	40	—	2	Cycloalkane (68); bicyclic-ether (7)	77
2.5 wt% Ru-2.5 wt% Cu/H-Y (2.6)	Water	3.3 wt% benzyloxy benzene (α-O-4)	523	40	—	2	Cycloalkane (56); cyclohexanol (24)	77
2.5 wt% Ru-2.5 wt% Cu/H-Y (2.6)	Water	3.3 wt% benzofuran (β-5)	523	40	—	2	Octahydrobenzofuran (85); cyclohexanol (8)	77
20 wt% Ni/H-ZSM-5 (45)	Water	Mixture of 4-*n*-propylphenol (10 mmol), 2-methoxy-4-*n*-propylphenol (10 mmol), 4-hydroxy-3- methoxybenzyl alcohol (10 mmol), 4′-hydroxy-3′-methoxyaceto-phenone (10 mmol) in 80 mL water	523	50	—	5	Hydrocarbon (25)	79
5 wt% Ni-5 wt% Fe/H-β	Water	Phenol (50 wt%), *o*-cresol (25 wt%) and guaiacol (25 wt%) 4 g in 100 ml water	573	16	—	4	Cycloalkane (22); aromatic hydrocarbon (29)	80

ZSM-5 supported Ru counterpart. Good catalyst stability, with no apparent loss of activity (conv. >95% and yield >85%) after 10 runs, was shown with the commercial ZSM-5 based catalyst. The stability of this Ru/ZSM-5 material was attributed to the favorable metal-support interaction between ruthenium and tetrahedral-coordinated framework Al in ZSM-5, which prevented the metal from sintering and leaching during catalysis. In addition, well-crystallized commercial ZSM-5 efficiently suppressed the deposition of coke species on the surface and channels of ZSM-5, compared to the mesoporous ZSM-5. This established example points to the importance of the precise metal-support interaction for the stability of the catalysts.

A combination of Brønsted acid sites with an active metal phase is beneficial for the LA-to-GVL conversion, but absolutely essential to further transform GVL to PA/PE, a reaction that also requires a higher temperature than the LA-to-GVL step. In 2010, Lange and co-workers first reported an interesting application for zeolite-supported metal catalysts for the production of a new class of cellulosic biofuels, namely valeric esters.[32] These valeric biofuels showed superior fuel properties over other bio-fuel candidates, and could be directly blended into both gasoline and diesel up to high blend ratios. The production of the pentanoic acid esters (PE) from LA involved a three-step process: (1) LA hydrogenation to GVL, (2) GVL hydrogenation to PA, and (3) finally PA esterification. The GVL-to-PA step is the most challenging one owing to the relatively high stability of GVL under hydrogenation conditions. It could nevertheless be successfully carried out with a Pt/H-ZSM-5/SiO_2 catalyst, prepared by incipient wetness (dry) impregnation. Particles of SiO_2-bound zeolites containing 25 wt% of H-ZSM-5 (Si/Al = 15) and 75 wt% of SiO_2 were impregnated with an $(NH_4)_2PtCl_4$ solution. This bifunctional catalyst was very effective for the production of PA from GVL, and high activity (differential PA productivity of nearly 2 $g_{PA}\ g_{cat}^{-1}\ h^{-1}$) and selectivity (>90%) were achieved at 523 K, 10 bar H_2 in continuous, high-pressure tubular reactor units. Importantly, this excellent catalytic performance could be retained for longer than 1500 h with intermittent catalyst regeneration by burning-off coke under a flow of H_2 or air at 673 K. No apparent loss of Pt and dealumination of the zeolite, limited decrease in support surface area and no measurable loss of mechanical strength of the catalyst extrudates were observed during the long-term operation, indicating excellent stability. No further information on metal particle size or location was reported. In the example above GVL would be mainly in the gas phase at 523 K, which condition is less challenging in terms of catalyst stability than reactions in the liquid phase. Yan *et al.* prepared a Pd/H-Y (5 wt%, Si/Al = 2.6) catalyst *via* wet impregnation proved highly active (99% conversion of GVL, 60.6% yield of pentyl valerate (PV) and 22.9% yield of pentane) at 533 K and 80 bar H_2 in octane in a batch reactor. However, catalyst deactivation was already observed in the second run under the applied conditions, owing to aggregation of metal particles and coke deposition on the surface.[47]

Efficient combination of hydrogenation and acidic functions in zeolite-supported metal catalysts can also allow the

Table 4 HDO of triglycerides and fatty acids over metal/zeolite catalysts

Catalyst (Si/Al)	Solvent	Feed	T (K)	P (bar)	WHSV/ LHSV (h^{-1})	Time (h)	Hydrocarbon yield (%)	Isomerization selectivity (%)	Ref.
$NiMo_{3-x}$/SAPO-11 (20 wt% MoO_3 and 3.5 wt% NiO)	No solvent	Methyl laurate	598/ 648	40	5	—	99	5–60	95
7 wt% Ni/SAPO-11 (Si/Al = 0.11 and Al/P = 1)	No solvent	Methyl palmitate	493	20	—	6	98	3	96
9.3 wt% Ni/H-ZSM-5 (108)	Dodecane	Methyl stearate (5 mmol) in dodecane (45 g)	553	40	—	8	100	—	94
10 wt% Ni/H-ZSM-5 (45)	Dodecane	1.3 wt% stearic acid	533	40	—	8	99	7	89
10 wt% Ni/H-ZSM-5 (120)	Dodecane	1.3 wt% stearic acid	533	40	—	8	65	8	89
10 wt% Ni/H-ZSM-5 (200)	Dodecane	1.3 wt% stearic acid	533	40	—	8	60	6	89
5 wt% Ni/H-β (75)	Dodecane	1.3 wt% stearic acid	533	40	—	8	96	19	89
10 wt% Ni/H-β (75)	Dodecane	1.3 wt% stearic acid	533	40	—	8	100	12	89
5 wt% Ni/H-β (180)	Dodecane	1.3 wt% stearic acid	533	40	—	8	96	6	89
10 wt% Ni/H-β (180)	Dodecane	1.3 wt% stearic acid	533	40	—	8	98	5	89
5.2 wt% Ni/H-β	Dodecane	1.3 wt% stearic acid	533	40	—	2	100	2	21
35 wt% Ni/H-USY-4 (16)	Dodecane	7.7 wt% stearic acid	533	40	—	1	96	—	116
35 wt% Ni/H-USY-4 (16)	Dodecane	7.7 wt% methyl stearate, ethyl palmitate, isopropyl palmitate, palmityl palmitate, stearyl stearate	533	40	—	1	94, 88, 100, 89, 97	1, 1, 1, 1, 2	116
35 wt% Ni/H-USY-4 (16)	Dodecane	7.7 wt% palm oil	533	40	—	2	100	1	116
4 wt% Ni/H-ZSM-5 (105)	Decane	1.4 wt% palmitic acid	533	40	—	4	100	9	97
4 wt% Co/H-ZSM-5 (105)	Decane	1.4 wt% palmitic acid	533	40	—	4	100	34	97
0.3 wt% PtSn/SAPO-11 (0.1)	No solvent	methyl palmitate (0.5 g)	533	30	5	—	77	58	100
4 wt% Ni/H-ZSM-22 (37.5)	Decane	1.4 wt% palmitic acid	533	40	—	4	100	46	19
1 wt% Pt/SAPO-11–30 wt% Al_2O_3 (Si/Al/P = 1 : 5.4 : 3.6)	No solvent	Soybean oil (palmitic/stearic/oleic/linoleic/linolenic = 10.2 : 3.7 : 22.8 : 53.7 : 8.6)	630	40	1	—	100	63	98
7 wt% Ni/SAPO-11 (Si/Al = 0.11 and Al/P = 1)	No solvent	Palm oil	553	40	2	—	100	85	115
8 wt% Ni/SAPO-11-Al_2O_3 (30 wt% γ-Al_2O_3 as binder)	No solvent	Soybean oil (palmitic/stearic/oleic/linoleic/linolenic = 10.2 : 3.7 : 22.8 : 53.7 : 8.6)	643	40	1	—	100	87	99
1 wt% Pt/H-ZSM-5 (11.5)	Water	10 wt% jatropha oil	543	65	—	12	99	—	91
1 wt% Pt-20 wt% Re /H-ZSM-5 (11.5)	Water	10 wt% jatropha oil	543	65	—	12	80	—	91
1 wt% Pt/USY (3.2)	Water	10 wt% vegetable oil	573	65	—	12	87	—	91
10 wt% Ni/H-β(180)	Water	Microalgae oil (0.1 g) in water (100 mL)	533	40	—	8	78	—	89

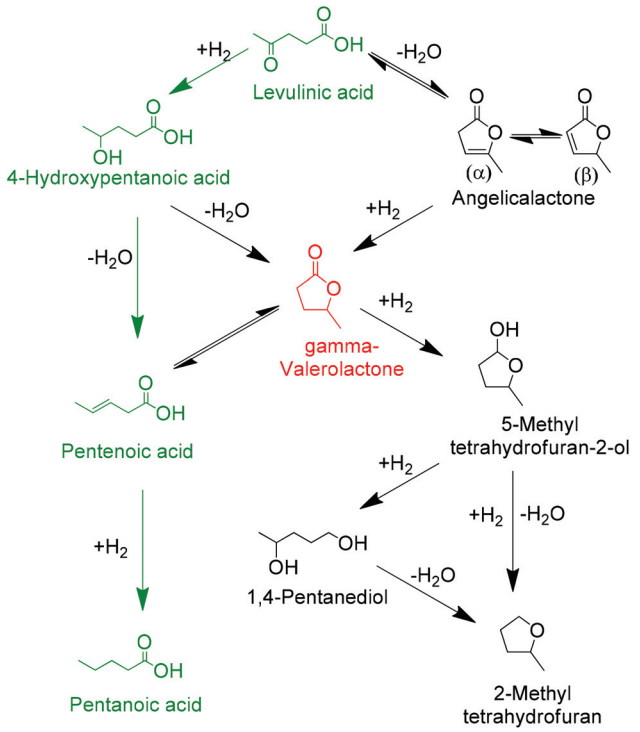

Scheme 1 Hydrodeoxygenation platform of levulinic acid.

series of reactions involved in the conversion of LA to PA/PE to be catalysed in one single step, potentially also under less severe reaction conditions. Indeed, Luo *et al.* first applied a bifunctional system for the direct, one-pot conversion of LA to PA without isolation of the GVL intermediate.[46] Expectedly, Ru-based zeolite supported catalysts proved better in the direct production of PA from LA than Ru/TiO_2, Ru/Nb_2O_5 catalysts at a fairly moderate temperature of 473 K. A Ru/H-ZSM-5 (1 wt%, Si/Al = 11.5) catalyst, prepared *via* wet impregnation using ruthenium nitrosyl nitrate, achieved a 45.8% yield of PA/PE from LA in dioxane at a reaction temperature of 473 K and 40 bar H_2 pressure, while the Ru/H-β prepared by the same method worked less well, with a 37.5% yield of PA/PE. The average diameter of the Ru particles in the catalyst was around 4 nm, suggesting them to be located at the external surface of zeolite. GVL ring-opening proved to be the rate-determining step on the pathway of direct conversion of LA to PA, necessitating strong Brønsted acid sites. This was in line with other reported observations that Brønsted acid containing bifunctional catalysts, for example, $Ru/SBA\text{-}SO_3H$, and a combination of Ni/SBA-15 and $SBA\text{-}SO_3H$, had the ability of direct hydrogenation of LA into PA.[48] Notably, the highly-oxygenated, polar and protic reaction medium proved corrosive and led to the deactivation of the Ru/zeolite materials in these liquid phase reactions. The gradual deactivation of Ru/H-ZSM-5 (Si/Al = 11.5) and Ru/H-β (Si/Al = 12.5) in 2-ethylhexanoic acid, used as an LA mimic to subject a catalyst to severe deactivating reaction conditions, and neat LA, was found to be mainly caused by support dealumination, and the inferior stability of the strong acid sites in Ru/H-β compared to Ru/H-ZSM-5 was demonstrated. Details of quantitative changes in aluminium speciation of Ru/H-β and Ru/H-ZSM-5 in 2-ethylhexanoic acid and neat LA during the reactions were revealed by FT-IR and ^{27}Al NMR, and the much more severe loss of strong acid sites in Ru/H-β compared to Ru/H-ZSM-5 was again illustrative for the inferior stability of the Ru/H-β.[49] Similarly, Kenichi *et al.* prepared a Pt/H-ZSM-5 catalyst *via* a wet impregnation approach for the one-pot conversion of LA to PA under similar conditions (2 or 8 bar H_2, 473 K). The catalyst was obtained *via* impregnation of H-ZSM-5 in an aqueous HNO_3 solution of $Pt(NH_3)_2(NO_3)_2$, and an average cluster size of 4.9 nm was achieved. A much higher yield of PA (78%) was obtained with Pt/H-ZSM-5 compared to that with physical mixture of Pt/SiO_2 and H-ZSM-5 (23%) under solvent free conditions. Efficient kinetic coupling of the metal and Brønsted acid site catalyzed steps was proposed to be behind the improved performance of the bifunctional material than a physical mixture. Catalyst stability again proved a challenge under these liquid phase reaction conditions. The Pt/H-ZSM-5 showed catalyst deactivation at the third consecutive runs, owing to Pt sintering and dealumination of ZSM-5 in pure LA during catalysis.[50] Other non-noble metal loaded ZSM-5 materials, such as Co and Ni on ZSM-5,[51,52] also showed good performance and stability in LA-to-PA conversion. Thus, ZSM-5 excels in providing Brønsted acidity and accessibility for short-chain platform molecules, and shows more potential in terms of catalyst stability and regeneration capacities. Normally, the bifunctional catalysts prepared by impregnation method inevitably suffer from metal sintering and leaching issues in the liquid phase reactions, resulting in deactivation of the catalysts. Interestingly, a stabilization strategy consisting of encapsulation of the metal particles into the zeolite crystal, was shown to be an efficient way of improving the catalyst stability for the direct conversion of LA into PA under severe reaction conditions (513 K and 30 bar H_2 in ethanol), with no apparent drop in catalyst performance through eight consecutive runs.[51] The encapsulation of metal particles inside the zeolite crystal limited metal migration and thus prevented metal aggregation and leaching during catalysis (Fig. 2). As the Brønsted acid sites are key for direct LA-to-PA conversion, their efficient preservation, both in amount and strength, upon metal loading, significantly influences the yield of target products (PA/PE) that can be obtained. Different extents of decrease in acid amount and strength have been observed upon addition of the metal by traditional impregnation and ion-exchange methods.[13,46] Choosing the right extraframework cation zeolite precursor and the proper metal salt, is known, for example, to determine to a great extent how well the strong acid sites are preserved. Further studies are still required to assess the influence of other preparation parameters of zeolite-supported bifunctional catalysts on acid site preservation.

Bifunctional catalysis with lignin-representative phenolics

Phenolics are widely investigated as aromatic model compounds for the upgrading of lignin and whole biomass derived

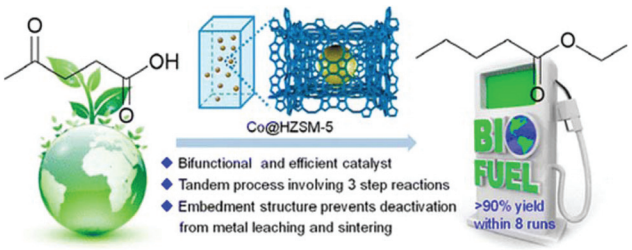

Fig. 2 Encapsulation of cobalt metal particles inside the zeolite for efficient production of valeric biofuel with improved catalyst stability, reproduced from ref. 51 with permission from [American Chemical Society], copyright [2014].

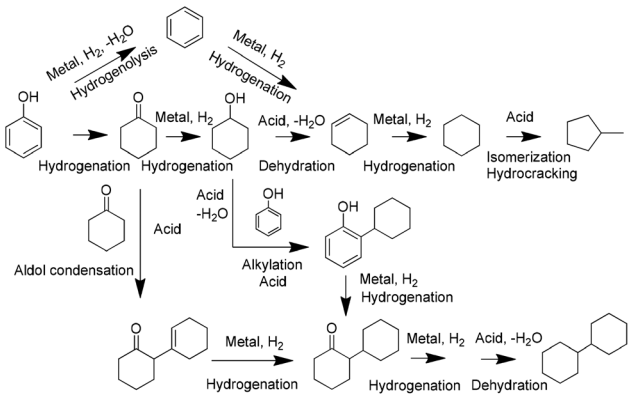

Scheme 2 Reaction pathways of phenol over zeolite-supported metal catalysts in catalytic HDO reactions.

bio-oils,[3,54,55] that can be produced for example by (catalytic) fast pyrolysis. Lignin, nature's dominant aromatic biopolymer, is one of major components in lignocellulosic biomass (15–30% by weight, 40% by energy). Phenolic-rich lignin fractions are becoming increasing available at low cost in agricultural products, municipal wastes, the pulp and paper industry and bioethanol refineries. Indeed, for reasons of economic viability, the development of lignin valorisation technologies is considered essential for the viable biorefinery operations.[56–58] Still, lignin is currently considered a waste product and used mainly for internal energy supply and as a source for producing low-grade fuels. To address this discrepancy, increasing attention is being devoted to catalytic upgrading of bio-oils and various lignin-derived phenolics.[18,58–60]

To better understand the reactions that occur and catalyst functions that are required during bio-oil production and upgrading, various oxygenated monoaromatics, such as phenol, anisole, guaiacol, catechol, eugenol and syringol have been used as model compounds.[61,62] The HDO of, *e.g.*, phenol typically involves a series of reactions, including direct hydrogenolysis to alkanes and hydrogenation, dehydration, cracking, (de)alkylation and hydrolysis steps, and various bifunctional catalysts have been recently evaluated for this reaction.[18,63–66] Zeolite-supported metal (Pt, Pd, Ni, Ru *etc.*) catalysts show particularly promising performance for HDO of phenol.[21,63,67–70] Phenol HDO is typically carried out at reaction temperatures in the range of 383 to 623 K with hydrogen pressures from 1 to 80 bar. Different HDO pathways of phenol that can occur over metal/zeolite catalysts are illustrated in Scheme 2. Phenol can be directly hydrogenolysed to benzene, and subsequently hydrogenated to cyclohexene, which can be further hydrogenated to cyclohexane, after which acid-catalysed isomerization can give methylcyclopentane. The direct hydrogenolysis pathway is dominant and is noticeably favoured at higher temperature conditions (>473 K).[64,71] Cyclohexane is favoured to form in batch reactors while benzene is preferred to form in continuous flow reactors owing to the shorter contact time that prevents further hydrogenation of aromatic ring. Alternatively, phenol can be hydrogenated first to cyclohexanone, and ultimately cyclohexanol and subsequently dehydrated to cyclohexene and then hydrogenated to cyclohexane, and finally to methylcyclopentane. Bicyclic products can be also formed from the coupling of two phenol-derived cycloalkanes over the bifunctional catalysts made with zeolites with large pores. For example, cyclohexanone can undergo aldol condensation and further HDO to give bicyclics; alternatively, phenol can be alkylated by cyclohexanol, *via* a carbenium intermediate to form 2-cyclohexylphenol, and then hydrogenated to bicyclics. In addition, other phenolic monomer compounds with additional functional groups, such as anisole, guaiacol, catechol, syringol and other intermediates have been also used to study the potential upgrading of lignin-derived monomers. HDO of those phenolics to hydrocarbons requires multi-step reactions to remove the additional oxygen functional groups *via* selective cleavage of C–O bonds (either demethoxylation or demethylation), hydrogenation, hydrolysis, and (de/trans) alkylation. Demethylation *via* the cleavage of C_{methyl}–O bond is typically favoured kinetically over direct deoxygenation, owing to C_{methyl}–O being weaker than the C_{aryl}–O one. Bifunctional catalysts can link these different reaction steps required for product formation. Metal sites can serve as the active sites for demethylation, demethoxylation, and hydrogenation, while acidic sites catalyze dehydration, hydrolysis and (de/trans) alkylation reactions.

Remarkable HDO efficiency could indeed be achieved by a combination of Brønsted acid and active metals. Yan *et al.* first showed that a homogeneous Brønsted acid (H_3PO_4) combined with a hydrogenation catalyst (Ru/C, Pd/C, Rh/C, Pt/C or metal nanoparticles) were effective for HDO of phenolics.[81,82] Nevertheless, the addition of homogeneous acids as catalysts will likely cause the recycling, corrosion and environmental problems. Therefore, the use of a solid zeolite support for the development of a metal/zeolite bifunctional catalyst system was proposed as an alternative for full HDO of phenolics. Pt/H-Y,[67,74,83] Pd/H-Y,[68] Pt/H-β,[61,75,83–85] Ru/H-β,[62] Ru/H-ZSM-5,[63] Pt/H-ZSM-5,[73,78] Ni/H-ZSM-5,[21,69,71,79] NiCo/H-ZSM-5,[64] and RuCu/H-Y[86] all showed excellent activity for the HDO of various phenolic monomers. Hong *et al.* reported that a Pt/H-Y conventionally prepared by impregnation, exhibited an excellent HDO activity (100%) and cyclohexane selectivity (>90%)

for phenol HDO in a fixed-bed configuration at 40 bar H_2 and 523 K. Pt supported on other zeolite supports (H-β and H-ZSM-5) were also tested and compared with the traditional sulfided CoMo catalysts, and the Pt/zeolite catalysts proved more efficient for the HDO of phenol, with both a higher activity and selectivity to cyclohexane even at high space velocity (20 h^{-1}).[67] Zhang *et al.* reported a Ru/H-ZSM-5 (Si/Al = 25), prepared *via* incipient wetness impregnation, which showed excellent HDO activity converting several lignin-related C_6–C_{10} phenolics to cyclohexane in high yield (>90%) in water at 473 K.[63] The high activity of the Ru/H-ZSM-5 was attributed to the strongly acidic Brønsted acid sites, as other acidic support such as SiO_2–Al_2O_3 delivered a much lower yield (~60%) with Ru and Rh, even at higher temperature (523 K).[87] Noble metal-based bifunctional catalysts such as Ru/H-β and Bifunctional metal/zeolite catalysts are also effective in HDO of phenolic dimers that mimic compounds that can be found in bio-oils and for which transformations require a tandem combination of metal/acid-catalyzed cleavage of C–O (4-O-5, α-O-5, β-1, β-5) and even C–C (5–5′, β–β) bonds and integrated hydrogenation, hydrogenolysis and dehydration reactions.[62,63,77,79,80] For example, the Ni/ZSM-5 catalyst, prepared by wet impregnation (average Ni particle size of 24 nm), was able to hydrodeoxygenate all major components of the aromatic fraction of pyrolysis bio-oil (substituted furans, mono- and dimeric-phenols), *via* a one-pot conversion at 523 K, 50 bar hydrogen pressure. The obtained O-free gasoline-range hydrocarbons contained less than 10% of C_5–C_6 paraffins and more than 90% of C_5–C_9 naphthenes and C_6–C_9 aromatic molecules, allowing direct blending with gasoline. The Ni/ZSM-5 catalyst did not deactivate over 5 consecutive runs, and limited Ni leaching was observed after 80 h in water. This supported zeolite catalyst thus proved rather stable under these hydrothermal conditions.[79]

While the examples above illustrate that bifunctional metal/zeolite catalysts show strong potential for application in the downstream processing of bio-oils and phenolics, a knowledge gap still exists for these reactions in terms of the relation between catalyst preparation and performance, including stability. Most reported metal/zeolite catalysts were synthesized by simple traditional impregnation methods, with the metal nanoparticles mainly ending up on the external surface of zeolites. Indeed, many other options remain to be explored in catalyst synthesis methods, and many different parameters can be modulated and further optimized during the preparation processes. In addition, while previous studies were mainly focused on catalyst activity/selectivity, stability received less attention, with the metal/zeolite catalysts often being limitedly characterized after reactions. Sintering/leaching of metal particles, dealumination/desilication of the zeolite and coke deposition can occur and cause catalyst deactivation in the liquid phase under the employed conditions. Thus, more research is required to allow rational development of bifunctional catalysts, which are not only efficient in conversion and selectivity, but also show long term stability in liquid phase and under the applied conditions (see also Challenge 2).

Bifunctional catalysis with triglycerides and fatty acids

Triglycerides and fatty acids, widely found (as constituents) in microalgae, vegetable oils and animal fats, are highly suited for advanced bio-fuel applications, given their long carbon chains. In addition to the obvious direct application of fatty acid esters as biodiesel, extensive research efforts have aimed at upgrading triglycerides and fatty acid into advanced deoxygenated biofuels, also with the use of bifunctional zeolite-supported metal catalysts.[88–91] Scheme 3 shows the reaction pathway for the HDO of triglycerides with metal/zeolite catalysts. It proceeds *via* an initial metal catalysed hydrogenation of unsaturated double bonds, and subsequent hydrogenolysis of saturated triglycerides to fatty acids and propane. The following HDO of the released fatty acids involves either direct decarboxylation to corresponding alkanes or hydrogenation of carboxylate to corresponding aldehyde. The resulting aldehyde can either be further decarbonylated to ultimately give the alkane or hydrogenated to the alcohol, followed by dehydration and hydrogenation. The formed long-chain alkanes can be isomerized and cracked into branched and shorter-chain alkanes. The hydrogenolysis, decarboxylation, decarbonylation and hydrogenation steps are typically carried out over the metal sites, while the acid sites of the zeolites enable the dehydration of alcohol intermediates, isomerization and hydrocracking of the formed long-chain alkanes.

Straight chain acids and their esters, such as stearic acid (ester) and palmitic acid (ester), are often used as model compounds for fatty acid and triglyceride HDO. Conventional hydroprocessing catalysts, such as sulfide-based $NiMo/Al_2O_3$ and $CoMo/Al_2O_3$, exhibit high activity but poor stability owing to sulphur leaching during the reactions, which not only contaminates the products but also results in a quick deactivation of the catalysts.[92,93] Compared to traditional hydrotreating temperatures (623–723 K), HDO with bifunctional catalysts can be run at considerably lower temperatures (<573 K), shows higher selectivity to the target linear hydrocarbons. Various

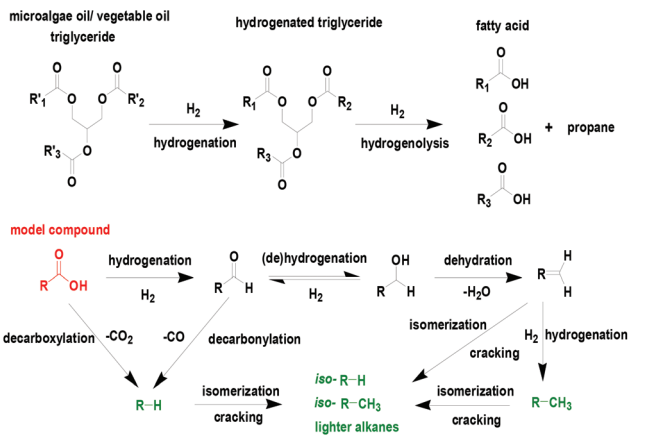

Scheme 3 Reaction pathway of transformation of triglycerides and fatty acids to alkanes in catalytic HDO reaction, (R′1, R′2 and R′3 are unsaturated alkyl chains), reproduced from ref. 89 with permission from [Wiley-VCH], copyright [2012].

metal/zeolite systems have been reported for this reaction, including triglyceride/or derivatives (vegetable, jatropha and microalgae oil) and fatty acid towards biofuel production, with metals ranging from Pt, Pd, to the base metals Ni, Co, and zeolites supports including ZSM-5, ZSM-22, SAPO-11, H-β, and H-Y.[21,89,91,94–97] Intriguingly, Song *et al.* explored the effect of different preparation methods of Ni/H-β on HDO of stearic acid and crude microalgae oil.[90] Ni/H-β prepared by deposition-precipitation (d = 2.5 ± 0.7 nm) and nanoparticle grafting methods (d = 3.9 ± 1.0 nm) demonstrated higher activity and stability upon recycling due to a better distribution of smaller Ni particles, compared to a catalyst prepared by impregnation (d = 24.7 ± 12.8 nm), as confirmed by TEM, IR of adsorbed CO, and TPR-H_2 measurements. Although the Ni/H-β prepared by ion exchange/precipitation methods (d = 2.6 ± 1.4 nm) showed good activity with a high initial reaction rate, a dramatic increase in Ni particle size as well as a drop in activity was observed upon recycling. A less uniform Ni particle size distribution led to the growth of larger particles at the expense of smaller ones through Ostwald ripening. In the best catalysts, small metal particles thus offered high catalytic activity, with a narrow particle size distribution ensuring good stability by minimizing the growth of larger particles.

For diesel or aviation fuel application, isomerisation to branched alkanes or cracking to short-chain alkanes is necessary to improve fuel properties. Normally, higher temperature promotes the isomerization/cracking reactions resulting in the increase in iso-alkanes/*n*-alkanes ratio and short-chain products, while lower temperature favors long-chain *n*-alkane selectivity. Compared to using only zeolite as the catalyst, the metal/zeolite system can improve the iso-products formation at a relatively lower temperature (513 K). For a good isomerization selectivity, a combination of a high hydrogenation activity with moderate acidity is required. Such high catalytic activity and isomerization selectivity have been reported for Ni/H-ZSM-5,[89,94] Ni/H-ZSM-22,[19] $NiMo_{3-X}$/SAPO-11,[95] Pt/SAPO-11,[98] Ni/SAPO-11,[99] Co/H-ZSM-5,[97] and PtSn/SAPO-11[100] for the quantitative conversion of various substrates like palmitic acid, methyl palmitate, palm oil, soybean oil, and vegetable oil. When combination of zeolite with strong acidity or non-optimal metal/acid balance, the degree of cracking is favored with products in aviation fuel range. The extent of cracking was found to be dependent on the acid site density and pore size of the zeolite. Severe cracking of the produced alkanes (43%) was achieved with Ni/ZSM-5 (10 wt%, Si/Al = 45) in stearic acid HDO in dodecane at 533 K, 40 bar H_2 for 6 h.[89] The higher acid site concentration and the narrower pores of Ni/ZSM-5, compared to those of Ni/H-β, led to a much higher cracking rate due to a higher effective residence time on the acid sites.

For HDO of fatty acid and triglycerides, small-sized metal particles together with good size uniformity in zeolites are preferred, which can efficiently improve the catalyst performance, and also suppress the polymerisation reactions towards coke. To this end, a relatively solvent-free method, named melt infiltration, shows an advantage for catalyst preparation over traditional impregnation and ion exchange, where water is normally employed as solvent for loading a metal onto the zeolite support. For example, Cao *et al.* compared melt infiltration, incipient wetness impregnation and wet impregnation methods for the preparation of Ni/ZSM-22 catalysts for HDO of palmitic acid.[19] This Ni/ZSM-22 material prepared by melt infiltration then outperformed its counterparts prepared by conventional impregnation methods in terms of activity and isomerization selectivity over a temperature range from 473 to 533 K and 40 bar. Improved dispersion of metal was observed for the melt-infiltrated Ni/ZSM-22 catalysts, probably owing to avoiding the competitive adsorption of solvent molecules on the zeolite supports. The improved metal dispersion significantly contributed to catalyst stability as well, as no obvious deactivation was observed over five recycle runs at 533 K.

Concept 2: balancing the metal and acid sites

As illustrated above, HDO normally requires multiple, mechanistically-different reactions that occur both in series and in parallel, requiring different catalytic functions to occur. To achieve high selectivity towards the targeted product, efficient coupling of these different reactions by finding an optimal balance of metal and acid functions is of utmost important. Given the typically highly reactive nature of the intermediates involved in HDO of biomass-derived substrates, such optimization is often a sensitive affair.

Site-ratio balancing for HDO of levulinic acid

For levulinic acid HDO, variation in the relative amount of acid and metal steers the reaction towards different products. If hydrogenation dominates in a metal/zeolite catalyst, mostly GVL is formed, while PA formation requires the acid to dominate. For instance, under the same reaction conditions (473 K, 40 bar H_2), a high selectivity of GVL (>98%) could be achieved with a Ru/H-ZSM-5 (Si/Al = 140) catalyst containing a low amount of acid, while a high selectivity of PA (91.3%) could be obtained with the more acidic Ru/H-ZSM-5 (Si/Al = 11.5).[13] Other products can be also obtained by well-tuning different functional sites. Proper addition of metal oxide as a promotor can also tune metal properties and enables a direct transformation of LA to MTHF *via* 1,4-pentanediol (1,4-PeD) in the HDO route.[101–103] A bimetallic Pt–Mo/H-β catalyst (3.9 wt% Pt and 0.13 wt% Mo), prepared by impregnation, was reported with a high MTHF yield of 86% for the one-pot hydrogenation of LA to MTHF using water as a solvent at 403 K and 50 bar H_2 for 24 h.[53] The Pt particles were found to have an average diameter of 7.1 nm, suggesting that they are mainly located on the external surface of zeolite; the MoO_x clusters were instead found to be highly dispersed on the surface of the H-β zeolite. Addition of MoO_x species to Pt nanoparticles efficiently improves the hydrogenation of LA to 1,4-PeD *via* a synergistic effect, while acidity of zeolite enables subsequent cyclodehydration of 1,4-PeD to MTHF. The nature of the metal also plays a role and normally higher metal loadings are required for non-noble

metals (10–30 wt%), such as Ni and Cu,[40,104] than for noble metals (<5 wt%) for LA to GVL conversions, owing to the intrinsic differences in hydrogenation ability. With the acid-catalyzed ring opening of GVL being rate determining in the GVL-to-PA conversion, the efficiency of this reaction was found to indeed correlate with zeolite aluminium content.[32,46,47,50,51] The zeolite with higher amount of aluminium is favoured for obtaining good catalytic performance, however, catalyst stability is a major concern when the high amount of aluminium presents in the zeolite structure. On the one hand, the presence of high amount of aluminium in framework will bring down the stability of the framework, resulting in a quick deactivation of the zeolite *via* dealumination, especially in liquid phase hydrothermal conditions. On the other hand, the high amount of aluminium also leads to higher amount of carbonaceous deposit formation during catalysis.

Site-ratio balancing for HDO of phenolics

An optimal balance between metal and acid for bifunctional catalyst is also pivotal to efficiently couple the various reactions in HDO of phenolics. For example, strongly acidic zeolites in combination with moderate hydrogenation activity are inclined to yield more alkylation products. For selective bicycloalkane production from coupling of phenolic monomer, an optimal metal/acid site balance (metal–acid mole ratio of 1 : 22) was achieved over Pd nanoclusters supported on H-β at 473–523 K using water as solvent. Yields of up to 80% of bicycloalkanes were attained for selective hydroalkylation and deoxygenation of substituted phenols. The Pd/H-β catalyst optimally adjusts the competing rates of metal catalyzed hydrogenation, acid-catalyzed dehydration and alkylation of phenol derivatives to C_{12}–C_{18} bicycloalkanes.[70] Alternatively, a combination of high hydrogenation activity and strong acidity in metal/zeolite catalysts normally leads to the formation of cycloalkanes in phenolics HDO. That strong acidity accelerates the dehydration step of cyclohexanol during HDO of phenolics, confirmed with various metal/zeolite systems, such as Ru/H-ZSM-5, Pt/H-Y and Ni/H-ZSM-5.[63,69,71,74,105] The zeolite catalysts with the lowest Si/Al ratio indeed proved to be most selective to cycloalkanes. However, strongly acidic catalysts can also catalyze the isomerization/cracking of cyclohexane to form methylcyclopentane, as well as the undesired deposition of coke, leading to faster deactivation of the catalyst.[71] To this end, an optimal balance between metal and acid for bifunctional catalyst is required to achieve a compromise between catalytic performance and stability. In line with this, an approach of using hybrid zeolite Y and alumina as support to tune the acidity of Pd-based catalyst has been reported.[68] The 20/80 mixed H-Y/Al_2O_3 supported Pd/H-Y-Al_2O_3, where Pd was deposited preferentially on the H-Y zeolite rather than on alumina, showed improved performance in phenol HDO at 523 K, 15 bar H_2 using octane as the solvent. The highest phenol conversion (63%), with good selectivity to cyclohexene and cyclohexane (95%), was achieved with this catalyst, values similar to those attained with a commercial NiMo/Al_2O_3-zeolite hydrocracking catalyst activated by sulfidation. In contrast, the more acidic Pd/H-Y showed a much lower activity and selectivity to cyclohexene and cyclohexane, and an increasing selectivity of methylcyclopentane was observed at 573 K and 623 K. In addition, catalyst deactivation was indeed faster with Pd/H-Y, owing to a significant amount (16.3%) of coke.

Site-ratio balancing for HDO of triglycerides and fatty acids

Triglycerides and fatty acids are structurally related to the long-chain hydrocarbons in oil refineries. In the latter operations, efficient fuel production from long-chain alkanes is well-known to rely on properly balanced active sites in bifunctional hydroprocessing catalysts, with the strength and amount of hydrogenation (metal) and cracking/isomerization activity (acid) controlling the product distribution. Normally, strongly acidic zeolites with moderate hydrogenation activity result in formation of lighter products and gasoline, while more weakly acidic zeolites in combination with strong hydrogenation activity lead to longer-chain distillates.[106] Analogously, more acidic zeolites and non-optimal metal loading promote cracking activity, correlations which are also expected to hold for triglyceride and fatty acid HDO. Peng *et al.* studied moderate hydrogenation metal Ni-based zeolite catalysts with different Si/Al ratios for HDO of fatty acids. Full conversion of stearic acid was achieved with Ni/H-ZSM-5 (10 wt%, Si/Al = 45) in dodecane at 533 K and 40 bar H_2 for 6 h, but severe cracking (43% selectivity towards cracked alkanes was observed with such strong acidity). Upon increasing the Si/Al ratios of the Ni/H-ZSM-5 catalyst to 120 and 200, lower activities but less cracking were obtained, together with increased selectivity to long chain alkanes (84% and 93%, respectively).[89] Similarly, the strongly acidic Pt/H-ZSM-5 (1 wt%, Si/Al = 11.5) also showed a severe cracking (>50%) trend for HDO of jatropha oil at 543 K.[91]

Medium acidity with medium hydrogenation sites can shift the selectivity towards isomerization to branched alkanes, which is also required for high quality fuel. For example Zuo *et al.* prepared Ni catalysts with various supports (γ-Al_2O_3, SiO_2, SAPO-11, H-ZSM-5, and H-Y) by incipient wetness impregnation for the HDO of methyl palmitate to diesel.[96] The Ni/SAPO-11 catalysts with medium acidity showed superior performance, providing a proper balance between the Ni and acidic support. The influence of the ratio between these two was demonstrated by variation of the Ni loading from 2 to 9 wt%, with the 7 wt% Ni/SAPO-11 showing the highest hydrocarbon yield of 98% (93% for C_{15+} alkanes) at 493 K and 20 bar H_2.

Modification of metal with promoters on moderate acidic zeolites can further benefit the deoxygenation and isomerization selectivity. Chen *et al.* studied PtSn/SAPO-11 and $NiMo_{3-x}$/SAPO-11 bimetallic catalysts for the one-step conversion of methyl laurate to high branched isomer containing hydrocarbons.[95,100] A series of PtSn/SAPO-11 catalysts with 0.3 wt% Pt and atomic ratios of Sn/Pt from 1 to 3 were tested, with the highest HDO and isomerization selectivity being seen with a Sn/Pt ratio of 2 at 648 K and 30 bar H_2. The improved isomerization selectivity was assigned to a decrease in hydro-

genation ability upon addition tin, resulting in an increased formation and subsequent isomerization of unsaturated hydrocarbons. In another case, the strong cracking activity of Pt/H-ZSM-5 (1 wt%, Si/Al = 11.5, >50%) of jatropha oil at 543 K, could be suppressed by addition of rhenium to tune the surface acidity of Pt/H-ZSM-5 catalyst. An optimal Re/Al ratio of 0.8 was achieved for PtRe/H-ZSM-5 catalysts, with a high selectivity to long-chain hydrocarbon products (80% conversion and 70% C_{18} selectivity) even at a high jatropha/catalyst ratio of 10 at 543 K for 12 h.[91] Catalyst characterization indicated that Pt and Re were segregated on the surface of the PtRe/H-ZSM-5, but a synergy effect between the metals was postulated for the improved deoxygenation ability, however, without detailed explanation. The balance of metal and acid sites can be also tuned by variation of the synthesis process. The effect of changing the reduction temperature from 673 to 823 K on the structure and performance of a $NiMo_{3-x}$/SAPO-11 catalyst was investigated.[95] The $NiMo_{3-x}$/SAPO-11 catalyst reduced at 723 K exhibited an optimal balance between its metal function and preservation of amount of acid sites, thus offering a proper balance between its deoxygenation and isomerization activity.

Despite the important insights provided by the examples listed above, site-ratio balancing is still only limitedly studied in the HDO of biomass-derived platform and model compounds, and the general re-balance of different functional sites for achieving target products definitely needs further study, especially on how to rationally constitute the desired sites in one catalyst for efficient coupling kinetics of various reactions both in series and in parallel are required. Efforts also need to be made for understanding the insight for the significant rate enhancement, especially when a synergetic effect is proposed.

Concept 3: optimizing proximity between metal and acid sites

With respect to rational design of HDO catalysts, not only the ratio but also the proximity of acid site and metal hydrogenation function should be taken into account. There are normally two ways of proximity between metal and acid sites in metal/zeolite systems (Fig. 3). One is between the external metal particles and pore-mouth acid sites, the other is between metal clusters and acid sites confined in micropores of zeolites. Especially, the intimacy between metal and acid sites inside the micropores of zeolites can provide additional benefits and sometimes synergistic effects in catalysis. For example, metal stability can be significantly improved, owing to the constraint of the micropores, which suppresses the further growth and migration of metal clusters; in addition, the acid sites in the micropores might serve as the anchoring sites for the metal, and the strong interactions between metal and acid can efficiently prevent sintering and leaching; moreover, the nearby metal sites can quickly hydrogenate unsaturated intermediates, avoiding further transformation to carbonaceous deposits on acid sites; furthermore, a properly selected pore structure can efficiently stabilize the reactive intermediates *via* confinement effects, and the proximal metals confined in these pores can selectively hydrogenate the intermediates to target products.

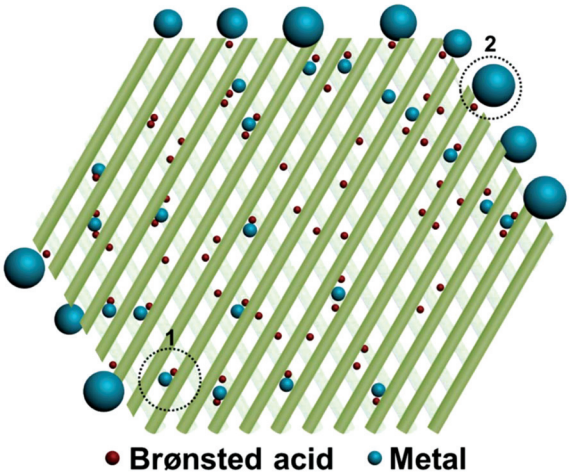

Fig. 3 Schematic representation of proximity between metal and acid sites in metal/zeolite catalysts. The blue spheres represent metal clusters, and the red spheres represent acid sites in the micropores. Two types of the intimacy between metal and acid sites are exhibited for metal/zeolite catalysts. 1 indicates a close proximity bwteen metal and acid sites confined in the micropores, and 2 indicates a close proximity between the external metal particles and acid located at pore mouths.

Site intimacy for HDO of levulinic acid

By exploring various synthesis parameters (metal precursor, cation type, reduction atmosphere) in the preparation of Ru/H-ZSM-5, controlled deposition/exchange of ruthenium into the ZSM-5 pores could be achieved *via* a combination of the wet impregnation and ion-exchange methods.[13] As a result, the Ru/H-ZSM-5 material with the highest amount of metal sites in close proximity to the acid sites in the micropores showed an excellent yield of 91.3% PA in the direct conversion of LA at 473 K and 40 bar H_2 pressure after 10 h, while the Ru/H-ZSM-5 with metal sites on the external surface of zeolite showed only a PA yield of 45.8%.[46] Key to localizing the metal close to the acid was the use of the ammonium form of ZSM-5, $Ru(NH_3)_6Cl_3$ as the ruthenium precursor, evaporation of the impregnation solvent at a proper rate and, finally, applying a direct reduction step at a slow heating ramp under a dilute H_2 flow. Together, this allowed for preservation of strong acidity and increased proximity between metal and acid function in the pores of zeolite. In this case, the entire cascade reactions can be processed inside the pores of the zeolite. LA is first hydrogenated to 4-hydroxypentanoic acid (HPA) over the metal sites, with the pores of ZSM-5 stabilizing the reactive intermediate HPA confinement, after which HPA is directly dehydrated to PEA, and finally hydrogenated to PA (green route in Scheme 1), avoiding ring closure to GVL. Characterization by TEM and physisorption indeed showed the Ru to be finely

(1.7 ± 0.4 nm) with a significant fraction of metal localized inside the pores of ZSM-5. Compared to the metal particles on the external surface of ZSM-5, the metal inside the zeolite microporous is more stably anchored *via* a strong interaction between metal cation and the negatively charged framework of the zeolite. Indeed, a bimodal particle size distribution (small particles <2 nm in the pores and larger particles from 5 to 14 nm on the external surface) was observed after recycle runs, indicating that sintering of metal could be mainly attributed to the agglomeration of the particles on the external surface of ZSM-5. Deactivation of this Ru/H-ZSM-5 material in recycle tests was primarily caused by carbon residue deposition on the acid sites. Less coke deposition was observed for the Ru/H-ZSM-5 with the metal dispersed into the micropores compared to a Ru/H-ZSM-5 material containing big particles (~4 nm) on the external surface of zeolite.

Close proximity between metal clusters and acid in zeolites can be also achieved by atomic layer deposition (ALD). Recently, Gu *et al.* employed ALD to deposit Pt into microporous H-ZSM-5 (Si/Al = 50).[23] The highest TOF (6.3 s^{-1}) was achieved with Pt/H-ZSM-5 prepared by the lowest ALD cycle number in aqueous-phase hydrogenation of LA to PA at 10 bar H_2 at 473 K. Upon increasing ALD cycle numbers, a decrease in TOF was correlated to a decrease in the amount of Pt species located close to acid sites in the pores of zeolite and an increase in the amount of Pt nanoparticles deposited on the external surface of ZSM-5. The Pt located in micropores could more efficiently affect the cascade reactions involved in PA production than the Pt located on the external surface of H-ZSM-5. Compared to a Pt/H-ZSM-5 catalyst prepared by impregnation, the Pt/H-ZSM-5 prepared by ALD showed better performance not only in terms of activity and selectivity, but also stability.

Site intimacy for HDO of phenolics

Close proximity between acid and metal sites can not only efficiently couple a series of reactions catalyzed by shortening the diffusion distance, but also promote the reaction rate *via* a synergistic action with both functions, in this respect, synergy effect on bifunctional zeolite-supported metal catalysts can be expected for HDO of phenolic model compounds. For catechol HDO reaction at 473 K, 30 bar H_2, the Ni/H-ZSM-5, with a much higher TOF, showed significant rate enhancement in hydrogenation and hydrogenolysis compared to H-ZSM-5 or Ni/SiO_2 catalysts. This prominent increase is tentatively attributed to the combination of a higher concentration of the reacting substrate and an additional delivery of hydrogen through protons from the proximal Brønsted acid sites.[12]

Notably, Zhu *et al.* demonstrated a synergistic effect in Pt/H-β (Si/Al = 19) for HDO of anisole into BTX (benzene, toluene and xylenes) at 673 K and 1 bar H_2 pressure.[84] High dispersion of Pt with an average particle size of 1.4 nm was obtained *via* incipient wetness impregnation, with a significant fraction of Pt being into the micropores of H-β. Pt clusters nearby the acid sites in the zeolite significantly improved both transalkylation of the methyl group to the phenolic ring and HDO reactions

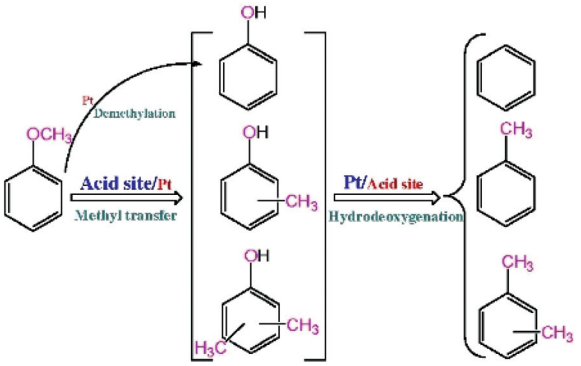

Scheme 4 Reaction pathway of HDO of anisole over Pt/H-β, reproduced from ref. 84 with permission from [Elsevier], copyright [2011].

than the monofunctional catalyst, observed with low consumption of hydrogen and minimized carbon loss as methane (Scheme 4). The metal sites promote the rate of cleavage of $O–CH_3$ and thus synergistically improve the overall rate of Brønsted acid catalyzed transalkylation reactions. Such rate enhancement was speculated to be owing to a partial hydrogenation of the phenolic ring near the C_{aryl}–OH bond on Pt that inhibited the delocalization of O lone pair orbital with the phenolic ring π bond orbital, followed by fast dehydration over the proximal Brønsted acid site, reforming the aromatic system. Meanwhile, the stability of the Pt/H-β is also improved with less coke formation. Later, Zhu *et al.* extended the Pt/H-β catalyst for HDO of *meta*-cresol under same conditions.[83] Pt/H-β showed a 10-fold increase in activity compared to that of Pt/SiO_2 toward HDO, with a three times increase in turnover frequency on the basis of Pt only, which indicated the synergistic effect of acid sites on the metal-catalyzed HDO reactions of phenolics. Meanwhile, good catalyst stability was also indicated for Pt/H-β during stability test and coke analysis. Compare to Pt/SiO_2, Pt/H-β showed comparable coke formation, but with significant higher activity.

Site intimacy for HDO of triglycerides and fatty acids

Triglycerides and fatty acids, holding long linear hydrocarbon chain, are too bulky to easily access into the micropores of zeolite materials. Accordingly, limited examples have been reported on building proximity between metal and acid sites inside the parent zeolite micropore systems for HDO of triglycerides and fatty acids. Still, site intimacy of some metal and acid sites can be built inside zeolite *via* introducing mesopores or outside zeolite *via* making nano-structured zeolites (see also in Challenge 1). Once the diffusion limit is overcome, the beneficial effect in coupling of different tandem reactions involved in HDO of triglycerides and fatty acids can be expected, however, the stability of such zeolite catalysts might face a high level of risk, especially under hydrothermal and liquid phase conditions. Therefore, the catalyst 'teetertotter' between 'accessibility' and 'stability' needs to be well balanced by designing well-defined structure of catalysts, which provides

the right proximity of distinct sites and stable structure, *via* rational synthesis approaches.

Indeed, more control over catalyst synthesis is further required to achieve the desired proximity between the metal and acid sites. Synergistic effect arised from proximity/intimacy between metal and acid sites for biomass HDO reactions is still limitedly studied, and more insight is required to understand the origin of these synergistic effects. In addition, the role of confinement effects on catalytic performance of zeolite, especially in the liquid phase, is still vague and very limited studied.

Concept 4: exploiting shape selectivity

Shape selectivity in zeolite catalysis has been studied and exploited in both academia and industry for almost 60 years. The shape, or topology, of the internal pore structure of a zeolite has been shown to have a great impact on tuning product distribution, allowing particular selectivity to be imposed by the zeolite, *e.g.* on isomerization and cracking reactions. As such, it has had a significant impact on the design of new catalytic processes in petrochemistry and refining.[107–109] As expected from the increasing application of zeolites in biomass conversion, shape selectivity effects can be seen in various biorefinery processes, including the bifunctional catalyst materials used for upgrading of bio-derived platform molecules and model compounds. Philippaerts *et al.* reported a shape selective Pt/Na-ZSM-5 catalyst, which could efficiently discriminate between the linear *trans*- and bent *cis*-unsaturated fatty acids, selectively converting the undesired *trans*-isomers by room-temperature adsorption and hydrogenation.[110] The optimal Pt/Na-ZSM-5 catalyst was obtained by competitive ion-exchange using a Na/Pt atomic ratio of 25 and subsequent calcination at 623 K with a slow heating ramp in a high O_2 flow. This procedure ensured a homogeneous Pt-distribution (1.7 nm) in the zeolite, which was found to be the most important preparation parameter to achieve good shape selectivity, even after reduction in H_2. Moreover, the Pt/Na-ZSM-5 material also exhibited excellent shape-selective hydrogenation of model triacylglycerols, preferring hydrogenation of the *trans*-over the *cis*-fatty acid chains.[111] In this case, the middle chain of the triglyceride was preferably reduced, which was attributed to pore mouth adsorption of the substrate in a tuning fork configuration. The selective hydrogenation and removal of undesired *trans*-isomers resulted into the production of desirable and healthy fats/oils (low in *trans*, high in oleic).

Differently sized zeolite micropores can also provide different extents of spatial constraints on molecular motion and product formation, which can provide a shape selectivity effect on the product distribution. In the HDO of phenolic monomers to alkanes over metal/zeolite catalysts, the shape selectivity concept has thus been applied to tune product selectivity. Monocycloalkanes are the main product when using a small pore zeolite, such as H-ZSM-5;[67,72,112,113] While bicycloalkanes can be selectively produced when using a large pore zeolite supported bifunctional catalyst, such as H-Y and H-β.[67,72,113,114] Notably, during HDO of bulky model compounds of fatty acid esters and different oil (soybean/vegetable/palm/jatropha oil), the narrow channels of 10-ring zeolites also show a good product selectivity of diesel range products. The cracking of bulk molecules started at these acid sites at the pore mouth of 10-ring zeolites, and consequent upgrading steps could be thus followed with the resulting small species diffusing into the zeolite pores. For example, Pt/SAPO-11-Al_2O_3 (30 wt% γ-Al_2O_3 as a binder),[98] Ni/SAPO-11,[96,99,115] Pt/H-ZSM-5,[91] and $NiMo_{3-x}$/SAPO-11[95] can selectively upgrade various fatty acid esters and different oil (soybean/vegetable/palm/jatropha oil) into diesel range products, with excellent catalytic activity and high isomerization selectivity.

Challenge 1: accessibility of active sites

In order to overcome diffusion, adsorption and desorption limitations, improvement of accessibility of active sites of zeolite crystals can be achieved *via* two approaches (Fig. 4). One is introducing mesopores into the zeolite framework, to achieve hierarchical porosity in the zeolites. The hierarchical zeolite applied in biomass conversion has been reviewed extensively by Ennaert *et al.*[16] Such hierarchical zeolites facilitate the diffusion of molecules in and out of the zeolite crystal and enlarge the amount of accessible active sites. The other approach is to decrease the size of zeolite crystal, *i.e.* by making nano-structured zeolites. The nano-structured zeolite can efficiently shorten the diffusion distance inside the zeolite crystal and expose more surface active sites compared to the parent zeolites. Metals supported on such zeolites should be more accessible than metals in the pores or on the external surface of conventional zeolites. For both approaches, promising results have been obtained in a large variety of reactions in petrochemistry,[117,118] and much can be expected when this approach is extended to zeolite supported metal catalysts used for HDO reactions of bio-derived compounds, where bulky molecules are often involved.

For example, a mesoporous ZSM-5 supported Pt catalyst showed enhanced performance of the upgrading of bio-oil model compounds (dibenzofuran, cresol and guaiacol) compared to a traditional ZSM-5 supported Pt, which was attribu-

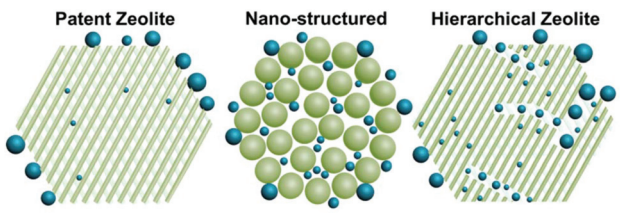

Fig. 4 Schematic representation of parent zeolite, nano-structured and hierarchical zeolites supported metal catalysts. The blue spheres represent metal clusters.

ted to reducing diffusion and adsorption limitations.[76] Similarly, an improved catalytic HDO performance has also been reported with Pt/Meso-β for upgrading phenolic monomer compounds (phenol, guaiacol).[75,119] In addition, hierarchisation of zeolites can also improve metal dispersion into the zeolite crystal, which can subsequently enhance the catalytic performance of HDO reactions in biomass conversion. An improved metal dispersion even at high metal loadings can be obtained with mesoporous zeolite as the support. Ma *et al.* prepared a high-metal content 35 wt% Ni/H-USY (Si/Al = 16) with small Ni nanoparticles (5 nm) loaded onto the hierarchical H-USY zeolites by the deposition-precipitation. This catalyst showed high efficiency in HDO of fatty acid, fatty esters and palm oil at 533 K, 40 bar H_2, with dodecane as the solvent. A high initial rate of 60 h^{-1} and a high C18 alkane selectivity of 96% from stearic acid were achieved, owing to the enhanced Brønsted acidity by adjacent Lewis acid resulting from a desilication treatment, and the significant amount (35 wt%) of highly dispersed Ni nanoparticles (4.9 ± 1.2 nm) onto/into the interconnected pores of hierarchical H-USY.[116]

The use of nano-structured zeolites as support for bifunctional catalysts can be also an efficient approach to improve accessibility limitations. In particular for those reactions that predominantly occur on the external surface of the zeolite, as is often the case in biomass conversion, the use of nano-sized structures can be particularly advantageous given the relatively large exposed external surface, offering abundant active sites. For example, Liu *et al*. reported a nano-sized SAPO-11 (Si/Al = 0.11 and Al/P = 1) supported Ni catalysts for the one step HDO of palm oil at 553 K, 40 bar H_2, and a high yield (80%) of liquid hydrocarbons, high isomerization selectivity (80%) and excellent stability were obtained.[115] The employment of the nano-sized SAPO-11 (20–50 nm) as the support significantly facilitated the diffusion of the bulky palm oil substrate. Similarly, the influence of support composition and morphology on the intrinsic activity of Ni supported on H-ZSM-5 was explored by Schreiber *et al.* in the HDO of methyl stearate at 553 K and 40 bar H_2.[94] Self-pillared zeolite nanosheets (with height of 8 nm and lengths of 20–100 nm) showed a significantly increased accessibility of acid sites by a factor of 3–4 and offered a one order of magnitude higher mesopore volume for metal deposition compared to conventional zeolite supports. Thus, higher Ni dispersion and higher reaction rates were reported for the nano-structured supports (TOF = 126 h^{-1}) than for the conventional zeolite (TOF = 94 h^{-1}).

A particularly important factor for zeolite-supported bifunctional catalysts in biomass conversion is the catalyst lifetime, as this is often rather limited owing to the coke deposition, and blockage of the zeolite micropores and active metal phase. Especially in condensed phase reactions with active, oxygen-rich intermediates, the micropores of the zeolites can be easily blocked by the carbonaceous deposits during reactions. Also here nano-structuring is advantageous, as the short microporous channels of a nano-structured zeolite allow for more facilely diffusion of the product out of the catalyst, and decrease the contact time of products with the active sites, thus avoiding secondary reaction that form carbonaceous deposits. In addition, such structure can also improve the metal dispersion, which can subsequently hydrogenate the unsaturated species and thus alleviate the coke formation. Excellent catalytic stability of Ni/nano-sized SAPO-11 catalysts was reported in HDO of palm oil, whereas a much lower amount of coke deposition was observed compared to a commercial Ni/SAPO-11, owing to a significant improvement of product diffusion and metal dispersion in the pores.[115]

While the examples above show potential, the employment of bifunctional, metal containing hierarchical or nano-structured zeolites for biomass conversion is limitedly studied. The optimal balance between introducing additional meso/macroporosity and maintaining the micropore size of zeolites has not been fully explored or achieved in many reactions in biomass valorization. A compromise between enhancing molecule diffusion, metal dispersion and accessibility of active sites, and maintaining the intrinsic acidity, space restriction, and shape selectivity of zeolites needs to be found to obtain enhanced catalytic performance. Therefore, tailored synthesis strategies (bottom-up and top-down) by carefully tuning various preparation parameters, such as conditions of steaming, acid/base leaching deserve more attention.

Challenge 2: stability of zeolite supported bifunctional catalysts

Most industrial zeolite supported bifunctional catalysts are normally employed for gas phase processes. When such catalysts are applied in biomass HDO reactions, normally in liquid phase, the oxygen-rich condensed phase and hydrothermal conditions (hot liquid water) can provide extra challenges for catalyst stability. Irreversible catalyst deactivation in HDO processes can occur *via* various pathways with metal/zeolite catalysts during catalysis. For example, it can be induced by the change of active metal phase (sintering, leaching and poisoning), destruction or alteration of the support (dealumination and desilication), or deposition of carbonaceous material (coke). Catalyst stability typically receives less attention than activity and selectivity, especially in more exploratory biomass conversion research. Thorough studies of zeolite-supported bifunctional catalysts are nevertheless essential to assess the efficiency of biomass HDO reactions.

Deactivation of the metal phase

The polar and acidic liquid solvent, reactants, formed intermediates and products can deactivate the metal phase of the bifunctional catalysts during the HDO conditions. Leaching or sintering of active metal are the main issues in polar and acidic oxygen-rich function reaction medium under hydrothermal conditions. The deactivation of metal phase in zeolite supported metal catalysts can be influenced by many different factors, including the size and the type of the metal particles and their interactions with the support. Strong interaction between metal and support, and uniform distribution of metal

dispersion can benefit the metal phase stability from alleviating metal leaching and sintering. Those are often correlated to the catalyst synthesis methods and post-synthetic modifications. A higher amount of Brønsted acid sites was shown to be useful for the formation of strong metal-support interactions in Ru/ZSM-5 (5 wt%, Si/Al = 25), and thus prohibited the Ru sintering and leaching at 343 K 30 bar H_2 in a 15 wt% levulinic acid aqueous solution.[45] The Ru/ZSM-5 catalyst, prepared by the wet impregnation method using commercial ZSM-5 support, showed a highly improved stability for the hydrogenation of levulinic acid in water, which can be reused for at least 10 times without apparent drop in activity (LA conv. >95%, GVL yield >85%).

At elevated temperature and more acidic reaction medium, the aggregation or overgrowth of metal nanoparticles can become more severe in liquid phase reaction, especially for the metal particles located on the external surface of zeolite. Different contents of metal sintering have been observed with Ru/zeolite catalysts, at 473 K, 40 bar H_2 after 10 h reactions in dioxane,[13] 2-ethylhexanoic acid and neat LA.[46] A bimodal distribution of the spent Ru/ZSM-5 points to the fact that the fraction of Ru metal particles located inside the zeolite is more resistant to sintering owing to the spacial constraint of zeolite pores, while the Ru particles located on the external surface of zeolite is facilely to form big particles under the applied conditions. The addition of a second metal to form alloy is also an efficient approach for improving metal phase stability, which can significantly improve the metal dispersion and alleviate metal aggregation issue.[38,120,121] Thuan Minh *et al.* studied HDO of phenol with bimetallic Ni-based/H-ZSM-5. Transition metal of Cu or Co was added in Ni/H-ZSM-5 for HDO of phenol at 523 K and 50 bar H_2. The addition of Cu to Ni/H-ZSM-5 (17) strongly promoted Ni reducibility and leads to the formation of Ni–Cu alloy but decreased the amount of Ni sites as well as tended to segregate at the external surface of H-ZSM-5, and those effects finally lowered conversion and selectivity of HDO products; while the addition of Co led to finely dispersed Ni particles and the stabilization of the active sites by forming alloys. The optimized catalyst, 10 wt% Ni-10 wt% Co/H-ZSM-5 showed a hydrocarbon selectivity of 99% at quantitative conversion of phenol.[64] Wang *et al.* investigated Ru–M/H-Y (M = Fe, Ni, Cu, Zn), prepared by incipient wetness impregnation methods, for HDO of softwood lignin and several lignin model compounds at 523 K and 40 bar H_2. Bimetallic catalysts, especially 2.5 wt% Ru-2.5 wt% Cu/H-Y (2.6) exhibited higher HDO activity of guaiacol to hydrocarbons than Ru/H-Y. The addition of a 3d transition metal (Fe, Ni, Cu, Zn) with Ru prevent over-hydrogenolysis of the hydrocarbon products into gaseous products. Based on characterization, the addition of Cu to Ru tended to form smaller alloy clusters with narrow size distribution and small average size. Good dispersion of metal species without severe segregation was observed owing to alloy formation.[86]

Another approach for improving metal stability in zeolite is encapsulation of metal particles inside zeolite crystal. Compare to traditional metal/zeolite catalysts, the encapsulated metal in zeolite (metal@zeolite) alleviates the issues such as metal sintering and leaching during biomass platform HDO reactions. Sun *et al.* prepared a cobalt embedded zeolite catalyst Co@H-ZSM-5 (10 wt%, Si/Al = 38) by the *in situ* synthesis method, where Co nanoparticles were encapsulated during the nucleation and growth of ZSM-5.[51] Compared to Co/H-ZSM-5 prepared by incipient wetness impregnation method, the Co@H-ZSM-5 catalyst showed excellent stability for one-pot HDO of LA at 513 K and 30 bar H_2, which successfully avoided deactivation and showed >90% PA + PE yield within eight consecutive runs. This preparation strategy efficiently stabilizes the cobalt nanoparticles against metal sintering and leaching under liquid phase reaction conditions. Wang *et al.* successfully prepared a Pd@silicalite-1 by an encapsulation method from solvent-free crystallization of a solid mixture including Pd nanoparticles, amorphous silica, and organic structural directing agent. The Pd@silicalite-1 was highly active and excellent in selective hydrogenation of bio-derived furfural to furan, giving a high selectivity of 98.7% with furfural conversion of 91.3%. Notably, the Pd@silicalite-1 showed high regenerated activity and good stability of those encapsulate Pd nanoparticles. Even with calcination at 873 K for 4 h in air, the Pd nanoparticles still keep their Pd size distribution. In comparison, most of the Pd nanoparticles on the external surface of silicalite-1 zeolite aggregated to larger than 10 nm nanoparticles after the same treatment. This phenomenon was attributed to the unique core–shell structure of Pd@silicalite-1 zeolite, where the silicalite-1 shell prevented the migration and aggregation of Pd nanoparticles.[122]

Zeolite stability

The zeolite supports are traditionally often used as catalysts for gas phase processes in industrial application. With many of the biomass-derived platform molecules necessitating liquid phase reactions for further conversion, for reasons of lack of volatility and lack of stability at higher temperature, these new conditions bring about particular challenges with respect to the stability of the zeolites. In addition, some of these biomass platform molecules, such as levulinic acid, are organic acids, which bring additional options for zeolite deactivation, *e.g.* by Al extraction. When these corrosive molecules are used as reactants, or produced as intermediates or are targeted products, the reaction medium is, dependent on the concentration, acidic and corrosive which can bring significant challenges for the stability of the employed zeolites. Indeed, Luo *et al.* has shown that irreversible framework dealumination of the Ru/zeolites (H-ZSM-5 and H-β) occurred during the hydrogenation of levulinic acid at 473 K in different solvents.[46] Especially in the solvent of 2-ethylhexanoic acid, the ZSM-5 and H-β zeolites are strongly affected by framework dealumination. The acidic reaction medium induces the conversion of framework aluminium species (FAL) into extraframework aluminium (EFAL) species, besides an overall decrease in the amount of aluminium species. Further NMR and FT-IR data showed that deactivation was mainly attributed to leaching of Al of zeolites, and changes in the coordination of

specific Al species correlated well with prior observed changes in acid sites caused by Al leaching.[49] For Ru/H-ZSM-5, the symmetric, tetrahedral FAL species were found to be mainly converted into distorted tetrahedral FAL species, with limited loss of aluminum to the solution by leaching. A severe loss of both FAL and EFAL species into the liquid phase was observed for Ru/H-β instead. Similar zeolite dealumination was observed when the reaction was performed in neat levulinic acid, but, as the corrosive reactant levulinic acid disappeared upon reactions, the gradual dealumination of zeolite was less pronounced. Nevertheless, when the reaction solvent was changed from organic acids to dioxane, limit structural changes of zeolite could be observed, and the catalyst activity could be restored by carbonaceous residue burning-off procedure.[13] Those studies show that Al-rich zeolites have potential for reactions with organic acids in aqueous phase when less protic and polar reaction medium and mild temperatures are applied. Otherwise, working in other mild solvents shows little problems of zeolite.

Considering the influence of water on the stability of catalysts is also necessary under biomass processing conditions. The hot liquid water has a great impact on the crystallinity of zeolites. The elevated temperature leads to the increase in the equilibrium constant of water, as a result of a higher concentration of protons and hydroxyls. When the temperature increases, the equilibrium constant can increase from 10^{-14} at 298 K to 10^{-11} above 573 K.[123,124] This can significantly influence the acid–base equilibrium and hydrolysis of water, and the increased concentration of protons and hydroxyls in the liquid phase can dramatic change the catalyst stability. Ravenelle *et al.* showed that the stability of zeolites in hot liquid water highly depended on their framework type.[125] ZSM-5 was stable at 423 and 473 K independent of its Si/Al ratio, whereas various zeolite Y samples showed different extents of degradation which depends on their Si/Al ratio. The dominant degradation pathway of zeolite Y by condensed water mainly occurs through hydrolysis of Si–O–Si bonds rather than dealumination under steaming conditions. Malola *et al.* have investigated the influence of water on desilication and dealumination processes in CHA. The desilication is the dominant degradation under steaming conditions.[126] The stability is also strongly correlated with the zeolite topology. Zeolite with high framework density such as MFI and MOR are relatively stable up to 523 K, while topologies with low density such as BEA and FAU show destruction at 423 K. Lutz *et al.* investigated the treatment of various zeolites with liquid water for 72 h up to 513 K and showed that MFI and MOR zeolites were relatively stable under such treatment, while BEA and FAU underwent severe degradation.[127] These studies provide fundamental insight of liquid water impact on zeolite materials under the biomass processing conditions. More research has to be devoted to zeolite stability under hydrothermal and acidic conditions, to assist the transition to large applications of zeolites in biomass conversion reactions. Resembling the addition of rare-earth elements into Y zeolite can efficiently improve the catalyst stability in fluid catalytic cracking,[128] introducing rare earth elements into the small cages of zeolite can be an approach to prevent extensive degradation of zeolite, which can stable the whole zeolite framework with an increase in the hydrothermal stability of the zeolite.

The carbonaceous deposit formed during biomass conversion can also cover the active site of bifunctional catalysts, resulting in the deactivation. Normally, the formation of polymeric products from unsaturated species is catalysed on the acid site of zeolite. The addition of metal, where hydrogen can be activated, can suppress coke formation, owing to subsequent hydrogenation of unsaturated species. Indeed, the addition of Pt to H-β resulted in an improved catalyst lifetime in the conversion of phenolic model compounds.[83,84,128] Moreover, the proximity of metal and acid can further alleviate agglomeration of unsaturated intermediates and form less carbonaceous deposits. Ru/H-ZSM-5 with more fractions of Ru located inside the micropores formed less coke compare to that with most Ru nanoparticles located on the external surface of ZSM-5 for the one-pot HDO of LA to PA at 473 K, 40 bar H_2 for 10 h.[13] In addition, the addition of basic promoters can regulate the acidity and alleviate the deposition of heavy carbonaceous species. Sun *et al.* demonstrated that the addition of potassium into Ni/H-ZSM-5 could efficiently decrease the content of carbonaceous deposits for hydrogenation of levulinic acid into pentanoic acid/ester. The addition of potassium regulates the catalyst acidity and modified the coke components from heavier species (alkylated poly-aromatics) to the lighter ones (alkylated mono-aromatics). The optimum catalyst, $Ni/K_{0.5}$/H-ZSM-5, effectively prolonged the catalyst lifetime from 20 h to 80 h.[52]

Conclusions and future prospects

The application of metal/zeolite bifunctional catalysts for HDO of biomass-derived platform molecules and model compounds that mimic components of primary biomass conversion processes, has recently been receiving increased attention and has shown considerable promise. The multistep conversions that are typically required in these tandem or cascade conversions, involving reactive and unstable intermediates, requires careful balancing, localization and accessibility of the distinct types of sites in order to achieve high selectivity of the desired products. Rational design of bifunctional catalysts can be of great significance for developing of promising catalysts for HDO reactions in biomass conversion. Indeed, more research is needed to establish synthesis-structure-performance relationships explaining the proximity and site balancing, and provide pointers as to how to obtain the desired materials. Notably, new protocols to achieve ultra-fine metal particle dispersions in the zeolite pores have been reported, *via* encapsulation of the metal into the zeolite crystal during zeolite synthesis or *via* the transformation of 2D zeolite to a 3D one.[25,122,129] Such catalyst design strategies offer advantages in catalyst performance and can be extended to application in HDO of biomass conversions.

Although the success of combination of metal and Brønsted acidity has been shown for efficient coupling of different reactions involved in HDO of biomass, the exact working state and the nature of active sites in liquid phase are still not clear. The polar solvent can change the nature of metal and acid sites during reactions. To this end, the development of *in situ* characterization of active sites in such liquid phase is thus necessary for understanding the deep insight into the nature of active sites during catalysis. In addition, more attention needs to be paid on how to properly combine metal and acid sites in zeolite with an optimal site-ratio, since the optimal balance is a thin region and side reactions can easily occur when the desired active sites are less accessible in such complex reaction networks. Many bifunctional combinations have shown promising HDO activity with rate enhancement or a synergistic effect, however, the underlying details of how such effect of different function sites comes from the proximity between metal and acid with an optimal site-balance, has been limitedly studied and better insight into the reaction mechanisms involved needs to be provided.

Much less examples of shape selectivity are studied in biomass conversion than in petrochemistry. Originally, this concept was developed for gas phase reactions with zeolite as the catalyst, nevertheless, the biomass HDO reactions with zeolite supported bifunctional catalysts in liquid phase may introduce additional complexities or even new recognition in shape selectivity. Currently, limited knowledge on such concept in liquid phase reactions definitely deserves more thoroughly exploiting, better starting with platform molecules and model compounds.

Despite improving accessibility of active sites *via* hierarchical or nano-structured zeolites have been successfully shown in petrochemical processes, however, such approaches may not always work out with improved catalytic performance in biomass HDO. The use of hierarchical zeolite should be necessarily selected in a proper system. High polar and functionalized substrate and solvent are often used in biomass conversion, which can inhibit the desorption of the formed intermediates and products. Those unstable and active species may subsequently form long-chain carbonaceous deposit in the pores of zeolite, ultimately block the active sites and cease the activity. Thus, target products with less polar and functional group, such as aromatics or alkanes are suitable for hierarchical zeolites. The nano-structured zeolites also need to be carefully chosen with a proper reaction media, since the liquid phase reaction can bring additional challenge for zeolite stability. The employment of relatively mild reaction conditions, leading to no severe zeolite degradation, is necessary for the nano-structured zeolites. Otherwise, a much severe destruction of zeolite can occur with the nano-structured zeolite materials compared to the parent zeolites.

Most research to date focuses on the chemistry of the reactions and the (initial) activity and selectivity of the catalysts during HDO reactions, and much less attention is devoted to catalyst stability. In addition, extremely low concentration of biomass-derived model molecules or dilute solutions as the reaction substrates were applied and a high amount of catalyst was often loaded in academic cases, together with their short-term reaction time, thereby catalyst deactivation might not be critically addressed. Recently, Lange has reviewed catalyst deactivation issues referring to long-term operation in the upgrading of biomass feedstocks from an industrial perspective.[130] The recognition of the stability challenges and emphasis of their importance for the industrial deployment of biomass conversion processes is a first and necessary step in the emergence of a robust bio-based economy. Commercial zeolite catalysts are traditionally designed and used for gas phase processes at elevated temperature (>523 K) in oil refinery,[131,132] which does not necessarily imply that they also endure in liquid phase conditions (polar, aqueous and even corrosive) mostly applied in biomass conversion.[133] Investigations have already shown that degradation of zeolite could occur in liquid water at high temperature (>423 K), while steaming at the same temperature only limitedly affected the zeolite structure.[125,134–136] In addition, corrosive highly oxygenated function species, such as organic acid, could also be involved in biomass conversion, resulting in significant challenge in zeolite stability.[13,46] One approach to overcome those issues is using mild solvent with a low polarity instead of water. For example, when the solvent is changed from organic acids to dioxane during HDO of LA, limited zeolite dealumination is observed. Another approach for zeolite stabilization is surface modification through coating, *e.g.* with a carbon layer, oxide coating or anchoring hydrophobic species. For example, Zapata *et al.* functionalized the surface of zeolite Y with hydrophobic organosilane species to increase hydrophobicity, resulting in a significant improvement in stability compared to non-functionalized zeolite in hot liquid water and in two-phase water-decalin emulsions at 473 K.[136,137] Coating the hydrothermally unstable Si–O–Si surface with a thin-film niobia by atomic layer deposition was also shown to effectively inhibit the hydrolysis of the Si–O–Si and improve the hydrothermal stability for the transformation of GVL to PA.[138] Another option to improve the stability is by doping of rare earth cations into the pores of zeolite, which is used for improvement of thermal stability and increasing zeolite structure collapse temperature.[139] Still, research efforts are required to understand the deeper fundamentals of catalyst stability challenges, to develop creative and innovative approaches.

The use of metal/zeolites for HDO of biomass platform/model compounds is with a great potential for catalysis due to their abundance and tenability; in addition, much less impurity in the biomass feedstock such as N and S, compared to petrochemical feedstock, alleviates the poison effect on active sites of catalysts. The final goal is the development of competitive industrial processes based on biomass platform/model compounds that can be economically competitive and attractive. Resembling the development of catalysts applied in analogous processes in petrochemistry,[140] upscaling tests and addition of other additives, such as binders, catalyst matrix, fillers *etc.*, require further exploration and research solutions in rational design of bifunctional catalysts, as well as overcom-

ing the complex and important challenges in process engineering.

Conflicts of interest

There are no conflicts to declare.

Acknowledgements

W. L., A. W. and T. Z. acknowledge the National Key Projects for Fundamental Research and Development of China (2018YFB1501600 and 2016YFA0202801), the National Natural Science Foundation of China (21703238, 21690080, 21690084, 21721004, 21673228, 21802134) and the Strategic Priority Research Program of the Chinese Academy of Sciences (XDB17020100) for financial support. Dr Changzhi Li is acknowledged for fruitful discussions.

References

1 C. O. Tuck, E. Pérez, I. T. Horváth, R. A. Sheldon and M. Poliakoff, *Science*, 2012, **337**, 695–699.
2 M. Poliakoff and P. Licence, *Nature*, 2007, **450**, 810–812.
3 G. W. Huber, S. Iborra and A. Corma, *Chem. Rev.*, 2006, **106**, 4044–4098.
4 P. C. A. Bruijnincx and B. M. Weckhuysen, *Angew. Chem., Int. Ed.*, 2013, **52**, 11980–11987.
5 S. H. Krishna, K. Huang, K. J. Barnett, J. He, C. T. Maravelias, J. A. Dumesic, G. W. Huber, D. B. Mario and B. M. Weckhuysen, *AIChE J.*, 2018, **64**, 1910–1922.
6 M. Besson, P. Gallezot and C. Pinel, *Chem. Rev.*, 2014, **114**, 1827–1870.
7 J. J. Bozell, L. Moens, D. C. Elliott, Y. Wang, G. G. Neuenscwander, S. W. Fitzpatrick, R. J. Bilski and J. L. Jarnefeld, *Resour., Conserv. Recycl.*, 2000, **28**, 227–239.
8 J. J. Bozell and G. R. Petersen, *Green Chem.*, 2010, **12**, 539–554.
9 P. A. Jacobs, M. Dusselier and B. F. Sels, *Angew. Chem., Int. Ed.*, 2014, **53**, 8621–8626.
10 J. Zecevic, G. Vanbutsele, K. P. de Jong and J. A. Martens, *Nature*, 2015, **528**, 245.
11 E. T. C. Vogt and B. M. Weckhuysen, *Chem. Soc. Rev.*, 2015, **44**, 7342–7370.
12 W. Song, Y. Liu, E. Barath, C. Zhao and J. A. Lercher, *Green Chem.*, 2015, **17**, 1204–1218.
13 W. Luo, P. C. A. Bruijnincx and B. M. Weckhuysen, *J. Catal.*, 2014, **320**, 33–41.
14 P. B. Weisz, in *Advances in Catalysis*, ed. D. D. Eley, P. W. Selwood, P. B. Weisz, A. A. Balandin, J. H. De Boer, P. J. Debye, P. H. Emmett, J. Horiuti, W. Jost, G. Natta, E. K. Rideal and H. S. Taylor, Academic Press, 1962, vol. 13, pp. 137–190.
15 N. Batalha, L. Pinard, C. Bouchy, E. Guillon and M. Guisnet, *J. Catal.*, 2013, **307**, 122–131.
16 T. Ennaert, J. Van Aelst, J. Dijkmans, R. De Clercq, W. Schutyser, M. Dusselier, D. Verboekend and B. F. Sels, *Chem. Soc. Rev.*, 2016, **45**, 584–611.
17 X. Li, G. Chen, C. Liu, W. Ma, B. Yan and J. Zhang, *Renewable Sustainable Energy Rev.*, 2017, **71**, 296–308.
18 M. Saidi, F. Samimi, D. Karimipourfard, T. Nimmanwudipong, B. C. Gates and M. R. Rahimpour, *Energy Environ. Sci.*, 2014, **7**, 103–129.
19 Y. Cao, Y. Shi, J. Liang, Y. Wu, S. Huang, J. Wang, M. Yang and H. Hu, *Chem. Eng. Sci.*, 2017, **158**, 188–195.
20 R. Nares, J. Ramírez, A. Gutiérrez-Alejandre, C. Louis and T. Klimova, *J. Phys. Chem. B*, 2002, **106**, 13287–13293.
21 W. Song, C. Zhao and J. A. Lercher, *Chem. – Eur. J.*, 2013, **19**, 9833–9842.
22 S. M. George, *Chem. Rev.*, 2010, **110**, 111–131.
23 X.-M. Gu, B. Zhang, H.-J. Liang, H.-B. Ge, H.-M. Yang and Y. Qin, *J. Fuel Chem. Technol.*, 2017, **45**, 714–722.
24 N. Wang, Q. Sun, R. Bai, X. Li, G. Guo and J. Yu, *J. Am. Chem. Soc.*, 2016, **138**, 7484–7487.
25 L. Liu, U. Díaz, R. Arenal, G. Agostini, P. Concepción and A. Corma, *Nat. Mater.*, 2016, **16**, 132.
26 A. Kulkarni, R. J. Lobo-Lapidus and B. C. Gates, *Chem. Commun.*, 2010, **46**, 5997–6015.
27 M. Moliner, J. E. Gabay, C. E. Kliewer, R. T. Carr, J. Guzman, G. L. Casty, P. Serna and A. Corma, *J. Am. Chem. Soc.*, 2016, **138**, 15743–15750.
28 B. Girisuta, L. P. B. M. Janssen and H. J. Heeres, *Chem. Eng. Res. Des.*, 2006, **84**, 339–349.
29 B. Girisuta, L. P. B. M. Janssen and H. J. Heeres, *Ind. Eng. Chem. Res.*, 2007, **46**, 1696–1708.
30 D. W. Rackemann and W. O. S. Doherty, *Biofuels, Bioprod. Biorefin.*, 2011, **5**, 198–214.
31 D. M. Alonso, S. G. Wettstein and J. A. Dumesic, *Green Chem.*, 2013, **15**, 584–595.
32 J.-P. Lange, R. Price, P. M. Ayoub, J. Louis, L. Petrus, L. Clarke and H. Gosselink, *Angew. Chem., Int. Ed.*, 2010, **49**, 4479–4483.
33 W. R. H. Wright and R. Palkovits, *ChemSusChem*, 2012, **5**, 1657–1667.
34 L. E. Manzer, *Appl. Catal., A*, 2004, **272**, 249–256.
35 C. Xiao, T.-W. Goh, Z. Qi, S. Goes, K. Brashler, C. Perez and W. Huang, *ACS Catal.*, 2016, **6**, 593–599.
36 M. Sudhakar, V. V. Kumar, G. Naresh, M. L. Kantam, S. K. Bhargava and A. Venugopal, *Appl. Catal., B*, 2016, **180**, 113–120.
37 P. P. Upare, J.-M. Lee, D. W. Hwang, S. B. Halligudi, Y. K. Hwang and J.-S. Chang, *J. Ind. Eng. Chem.*, 2011, **17**, 287–292.
38 W. Luo, M. Sankar, A. M. Beale, Q. He, C. J. Kiely, P. C. A. Bruijnincx and B. M. Weckhuysen, *Nat. Commun.*, 2015, **6**, 6540.
39 F. D. Pileidis and M. M. Titirici, *ChemSusChem*, 2016, **9**, 562–582.
40 V. Mohan, C. Raghavendra, C. V. Pramod, B. D. Raju and K. S. Rama Rao, *RSC Adv.*, 2014, **4**, 9660–9668.

41 S. Ishikawa, D. R. Jones, S. Iqbal, C. Reece, D. J. Morgan, D. J. Willock, P. J. Miedziak, J. K. Bartley, J. K. Edwards, T. Murayama, W. Ueda and G. J. Hutchings, *Green Chem.*, 2017, **19**, 225–236.
42 O. A. Abdelrahman, A. Heyden and J. Q. Bond, *ACS Catal.*, 2014, **4**, 1171–1181.
43 A. M. R. Galletti, C. Antonetti, V. De Luise and M. Martinelli, *Green Chem.*, 2012, **14**, 688–694.
44 A. M. Robinson, J. E. Hensley and J. W. Medlin, *ACS Catal.*, 2016, **6**, 5026–5043.
45 B. Zhang, Q. Wu, C. Zhang, X. Su, R. Shi, W. Lin, Y. Li and F. Zhao, *ChemCatChem*, 2017, **9**, 3646–3654.
46 W. Luo, U. Deka, A. M. Beale, E. R. H. van Eck, P. C. A. Bruijnincx and B. M. Weckhuysen, *J. Catal.*, 2013, **301**, 175–186.
47 K. Yan, T. Lafleur, X. Wu, J. Chai, G. Wu and X. Xie, *Chem. Commun.*, 2015, **51**, 6984–6987.
48 T. Pan, J. Deng, Q. Xu, Y. Xu, Q.-X. Guo and Y. Fu, *Green Chem.*, 2013, **15**, 2967–2974.
49 W. Luo, E. R. H. van Eck, P. C. A. Bruijnincx and B. M. Weckhuysen, *ChemPhysChem*, 2018, **19**, 379–385.
50 K. Kon, W. Onodera and K.-I. Shimizu, *Catal. Sci. Technol.*, 2014, **4**, 3227–3234.
51 P. Sun, G. Gao, Z. Zhao, C. Xia and F. Li, *ACS Catal.*, 2014, **4**, 4136–4142.
52 P. Sun, G. Gao, Z. Zhao, C. Xia and F. Li, *Appl. Catal., B*, 2016, **189**, 19–25.
53 T. Mizugaki, K. Togo, Z. Maeno, T. Mitsudome, K. Jitsukawa and K. Kaneda, *ACS Sustainable Chem. Eng.*, 2016, **4**, 682–685.
54 S. Van den Bosch, W. Schutyser, R. Vanholme, T. Driessen, S. F. Koelewijn, T. Renders, B. De Meester, W. J. J. Huijgen, W. Dehaen, C. M. Courtin, B. Lagrain, W. Boerjan and B. F. Sels, *Energy Environ. Sci.*, 2015, **8**, 1748–1763.
55 S. Crossley, J. Faria, M. Shen and D. E. Resasco, *Science*, 2010, **327**, 68–72.
56 J. Zakzeski, P. C. A. Bruijnincx, A. L. Jongerius and B. M. Weckhuysen, *Chem. Rev.*, 2010, **110**, 3552–3599.
57 A. J. Ragauskas, G. T. Beckham, M. J. Biddy, R. Chandra, F. Chen, M. F. Davis, B. H. Davison, R. A. Dixon, P. Gilna, M. Keller, P. Langan, A. K. Naskar, J. N. Saddler, T. J. Tschaplinski, G. A. Tuskan and C. E. Wyman, *Science*, 2014, **344**, 1246843.
58 C. Li, X. Zhao, A. Wang, G. W. Huber and T. Zhang, *Chem. Rev.*, 2015, **115**, 11559–11624.
59 R. Rinaldi, R. Jastrzebski, M. T. Clough, J. Ralph, M. Kennema, P. C. A. Bruijnincx and B. M. Weckhuysen, *Angew. Chem., Int. Ed.*, 2016, **55**, 8164–8215.
60 Z. Sun, B. Fridrich, A. de Santi, S. Elangovan and K. Barta, *Chem. Rev.*, 2018, **118**, 614–678.
61 G. S. Foo, A. K. Rogers, M. M. Yung and C. Sievers, *ACS Catal.*, 2016, **6**, 1292–1307.
62 G. Yao, G. Wu, W. Dai, N. Guan and L. Li, *Fuel*, 2015, **150**, 175–183.
63 W. Zhang, J. Chen, R. Liu, S. Wang, L. Chen and K. Li, *ACS Sustainable Chem. Eng.*, 2014, **2**, 683–691.
64 T. M. Huynh, U. Armbruster, M.-M. Pohl, M. Schneider, J. Radnik, D.-L. Hoang, B. M. Q. Phan, D. A. Nguyen and A. Martin, *ChemCatChem*, 2014, **6**, 1940–1951.
65 C. Zhao, J. He, A. A. Lemonidou, X. Li and J. A. Lercher, *J. Catal.*, 2011, **280**, 8–16.
66 W. Wang, Y. Yang, H. Luo, H. Peng and F. Wang, *Ind. Eng. Chem. Res.*, 2011, **50**, 10936–10942.
67 D.-Y. Hong, S. J. Miller, P. K. Agrawal and C. W. Jones, *Chem. Commun.*, 2010, **46**, 1038–1040.
68 S. RSCEcheandia, B. Pawelec, V. L. Barrio, P. L. Arias, J. F. Cambra, C. V. Loricera and J. L. G. Fierro, *Fuel*, 2014, **117**, 1061–1073.
69 C. Zhao, S. Kasakov, J. He and J. A. Lercher, *J. Catal.*, 2012, **296**, 12–23.
70 C. Zhao, D. M. Camaioni and J. A. Lercher, *J. Catal.*, 2012, **288**, 92–103.
71 X. Zhang, T. Wang, L. Ma, Q. Zhang and T. Jiang, *Bioresour. Technol.*, 2013, **127**, 306–311.
72 C. Zhao, D. M. Camaioni and J. A. Lercher, *J. Catal.*, 2012, **288**, 92–103.
73 M. Hellinger, H. W. P. Carvalho, S. Baier, D. Wang, W. Kleist and J.-D. Grunwaldt, *Appl. Catal., A*, 2015, **490**, 181–192.
74 H. Lee, H. Kim, M. J. Yu, C. H. Ko, J.-K. Jeon, J. Jae, S. H. Park, S.-C. Jung and Y.-K. Park, *Sci. Rep.*, 2016, **6**, 28765.
75 E. H. Lee, R.-S. Park, H. Kim, S. H. Park, S.-C. Jung, J.-K. Jeon, S. C. Kim and Y.-K. Park, *J. Ind. Eng. Chem.*, 2016, **37**, 18–21.
76 Y. Wang, J. Wu and S. Wang, *RSC Adv.*, 2013, **3**, 12635–12640.
77 H. Wang, H. Ruan, M. Feng, Y. Qin, H. Job, L. Luo, C. Wang, M. H. Engelhard, E. Kuhn, X. Chen, M. P. Tucker and B. Yang, *ChemSusChem*, 2017, **10**, 1846–1856.
78 H. Ohta, K. Yamamoto, M. Hayashi, G. Hamasaka, Y. Uozumi and Y. Watanabe, *Chem. Commun.*, 2015, **51**, 17000–17003.
79 C. Zhao and J. A. Lercher, *Angew. Chem., Int. Ed.*, 2012, **51**, 5935–5940.
80 H. Shafaghat, P. S. Rezaei and W. M. A. W. Daud, *J. Ind. Eng. Chem.*, 2016, **35**, 268–276.
81 N. Yan, C. Zhao, P. J. Dyson, C. Wang, L. Liu and Y. Kou, *ChemSusChem*, 2008, **1**, 626–629.
82 N. Yan, Y. Yuan, R. Dykeman, Y. Kou and P. J. Dyson, *Angew. Chem., Int. Ed.*, 2010, **49**, 5549–5553.
83 X. Zhu, L. Nie, L. L. Lobban, R. G. Mallinson and D. E. Resasco, *Energy Fuels*, 2014, **28**, 4104–4111.
84 X. Zhu, L. L. Lobban, R. G. Mallinson and D. E. Resasco, *J. Catal.*, 2011, **281**, 21–29.
85 M. M. Yung, G. S. Foo and C. Sievers, *Catal. Today*, 2018, **302**, 151–160.
86 H. Wang, H. Ruan, M. Feng, Y. Qin, H. Job, L. Luo, C. Wang, M. H. Engelhard, E. Kuhn, X. Chen,

M. P. Tucker and B. Yang, *ChemSusChem*, 2017, **10**, 1846–1856.
87 C. R. Lee, J. S. Yoon, Y.-W. Suh, J.-W. Choi, J.-M. Ha, D. J. Suh and Y.-K. Park, *Catal. Commun.*, 2012, **17**, 54–58.
88 C. Zhao, T. Bruck and J. A. Lercher, *Green Chem.*, 2013, **15**, 1720–1739.
89 B. Peng, Y. Yao, C. Zhao and J. A. Lercher, *Angew. Chem., Int. Ed.*, 2012, **51**, 2072–2075.
90 W. Song, C. Zhao and J. A. Lercher, *Chem. – Eur. J.*, 2013, **19**, 9833–9842.
91 K. Murata, Y. Liu, M. Inaba and I. Takahara, *Energy Fuels*, 2010, **24**, 2404–2409.
92 S. T. Oyama, *Catal. Today*, 1992, **15**, 179–200.
93 T. R. Viljava, R. S. Komulainen and A. O. I. Krause, *Catal. Today*, 2000, **60**, 83–92.
94 M. W. Schreiber, D. Rodriguez-Nino, O. Y. Gutierrez and J. A. Lercher, *Catal. Sci. Technol.*, 2016, **6**, 7976–7984.
95 N. Chen, S. Gong and E. W. Qian, *Appl. Catal., B*, 2015, **174–175**, 253–263.
96 H. Zuo, Q. Liu, T. Wang, L. Ma, Q. Zhang and Q. Zhang, *Energy Fuel*, 2012, **26**, 3747–3755.
97 Y. Shi, E. Xing, Y. Cao, M. Liu, K. Wu, M. Yang and Y. Wu, *Chem. Eng. Sci.*, 2017, **166**, 262–273.
98 C. Wang, Z. Tian, L. Wang, R. Xu, Q. Liu, W. Qu, H. Ma and B. Wang, *ChemSusChem*, 2012, **5**, 1974–1983.
99 C. Wang, Q. Liu, J. Song, W. Li, P. Li, R. Xu, H. Ma and Z. Tian, *Catal. Today*, 2014, **234**, 153–160.
100 N. Chen, Y. Ren and E. W. Qian, *J. Catal.*, 2016, **334**, 79–88.
101 F. M. A. Geilen, B. Engendahl, A. Harwardt, W. Marquardt, J. Klankermayer and W. Leitner, *Angew. Chem., Int. Ed.*, 2010, **39**, 5510–5514.
102 P. P. Upare, J.-M. Lee, Y. K. Hwang, D. W. Hwang, J.-H. Lee, S. B. Halligudi, J.-S. Hwang and J.-S. Chang, *ChemSusChem*, 2011, **4**, 1749–1752.
103 L. Yuehui, T. Christoph, C. Xinjiang, J. Kathrin and B. Matthias, *Angew. Chem., Int. Ed.*, 2015, **54**, 5196–5200.
104 A. M. Hengne and C. V. Rode, *Green Chem.*, 2012, **14**, 1064–1072.
105 F. Anaya, L. Zhang, Q. Tan and D. E. Resasco, *J. Catal.*, 2015, **328**, 173–185.
106 W. Jens, *ChemCatChem*, 2012, **4**, 292–306.
107 B. Smit and T. L. M. Maesen, *Nature*, 2008, **451**, 671.
108 V. J. Frilette, P. B. Weisz and R. L. Golden, *J. Catal.*, 1962, **1**, 301–306.
109 P. B. Weisz, V. J. Frilette, R. W. Maatman and E. B. Mower, *J. Catal.*, 1962, **1**, 307–312.
110 A. Philippaerts, S. Paulussen, S. Turner, O. I. Lebedev, G. Van Tendeloo, H. Poelman, M. Bulut, F. De Clippel, P. Smeets, B. Sels and P. Jacobs, *J. Catal.*, 2010, **270**, 172–184.
111 A. Philippaerts, S. Paulussen, A. Breesch, S. Turner, O. I. Lebedev, G. V. Tendeloo, B. Sels and P. Jacobs, *Angew. Chem., Int. Ed.*, 2011, **50**, 3947–3949.
112 C. Zhao and J. A. Lercher, *ChemCatChem*, 2012, **4**, 64–68.
113 S. Kasakov, H. Shi, D. M. Camaioni, C. Zhao, E. Barath, A. Jentys and J. A. Lercher, *Green Chem.*, 2015, **17**, 5079–5090.
114 C. Zhao, W. Song and J. A. Lercher, *ACS Catal.*, 2012, **2**, 2714–2723.
115 Q. Liu, H. Zuo, T. Wang, L. Ma and Q. Zhang, *Appl. Catal., A*, 2013, **468**, 68–74.
116 B. Ma, X. Yi, L. Chen, A. Zheng and C. Zhao, *J. Mater. Chem. A*, 2016, **4**, 11330–11341.
117 M. S. Holm, E. Taarning, K. Egeblad and C. H. Christensen, *Catal. Today*, 2011, **168**, 3–16.
118 Y. Yan, X. Guo, Y. Zhang and Y. Tang, *Catal. Sci. Technol.*, 2015, **5**, 772–785.
119 J. Horáček, G. Šťávová, V. Kelbichová and D. Kubička, *Catal. Today*, 2013, **204**, 38–45.
120 A. Shrotri, A. Tanksale, J. N. Beltramini, H. Gurav and S. V. Chilukuri, *Catal. Sci. Technol.*, 2012, **2**, 1852–1858.
121 D. M. Alonso, S. G. Wettstein and J. A. Dumesic, *Chem. Soc. Rev.*, 2012, **41**, 8075–8098.
122 C. Wang, L. Wang, J. Zhang, H. Wang, J. P. Lewis and F.-S. Xiao, *J. Am. Chem. Soc.*, 2016, **138**, 7880–7883.
123 A. V. Bandura and S. N. Lvov, *J. Phys. Chem. Ref. Data*, 2006, **35**, 15–30.
124 A. A. Peterson, F. Vogel, R. P. Lachance, M. Fröling, J. M. J. Antal and J. W. Tester, *Energy Environ. Sci.*, 2008, **1**, 32–65.
125 R. M. Ravenelle, F. Schüßler, A. D'Amico, N. Danilina, J. A. van Bokhoven, J. A. Lercher, C. W. Jones and C. Sievers, *J. Phys. Chem. C*, 2010, **114**, 19582–19595.
126 S. Malola, S. Svelle, F. L. Bleken and O. Swang, *Angew. Chem., Int. Ed.*, 2012, **51**, 652–655.
127 W. Lutz, H. Toufar, R. Kurzhals and M. Suckow, *Adsorption*, 2005, **11**, 405–413.
128 E. F. Sousa-Aguiar, F. E. Trigueiro and F. M. Z. Zotin, *Catal. Today*, 2013, **218–219**, 115–122.
129 J. Zhang, L. Wang, B. Zhang, H. Zhao, U. Kolb, Y. Zhu, L. Liu, Y. Han, G. Wang, C. Wang, D. S. Su, B. C. Gates and F.-S. Xiao, *Nat. Catal.*, 2018, **1**, 540–546.
130 J. P. Lange, *Angew. Chem., Int. Ed.*, 2015, **54**, 13186–13197.
131 W. Vermeiren and J.-P. Gilson, *Top. Catal.*, 2009, **52**, 1131–1161.
132 A. Corma, *Chem. Rev.*, 1995, **95**, 559–614.
133 R. Rinaldi and F. Schüth, *Energy Environ. Sci.*, 2009, **2**, 610–626.
134 D. W. Gardner, J. Huo, T. C. Hoff, R. L. Johnson, B. H. Shanks and J.-P. Tessonnier, *ACS Catal.*, 2015, **5**, 4418–4422.
135 T. Ennaert, J. Geboers, E. Gobechiya, C. M. Courtin, M. Kurttepeli, K. Houthoofd, C. E. A. Kirschhock, P. C. M. M. Magusin, S. Bals, P. A. Jacobs and B. F. Sels, *ACS Catal.*, 2015, **5**, 754–768.
136 P. A. Zapata, Y. Huang, M. A. Gonzalez-Borja and D. E. Resasco, *J. Catal.*, 2013, **308**, 82–97.

137 P. A. Zapata, J. Faria, M. P. Ruiz, R. E. Jentoft and D. E. Resasco, *J. Am. Chem. Soc.*, 2012, **134**, 8570–8578.
138 Y. J. Pagán-Torres, J. M. R. Gallo, D. Wang, H. N. Pham, J. A. Libera, C. L. Marshall, J. W. Elam, A. K. Datye and J. A. Dumesic, *ACS Catal.*, 2011, **1**, 1234–1245.
139 F. E. Trigueiro, D. F. J. Monteiro, F. M. Z. Zotin and E. Falabella Sousa-Aguiar, *J. Alloys Compd.*, 2002, **344**, 337–341.
140 S. Mitchell, N.-L. Michels and J. Perez-Ramirez, *Chem. Soc. Rev.*, 2013, **42**, 6094–6112.